Characterizing biosignatures in coralloid speleothems from basaltic lava tubes in Lava Beds National Monument

Jenny Ni

Department of Earth and Planetary Sciences

McGill University, Montreal

August, 2019

A thesis submitted to McGill University in partial fulfillment of the requirements of the degree of Master of Science

Abstract

Coralloid speleothems or cave corals are secondary mineral deposits that resemble the form of a coral, and which develop through groundwater seepage, water-rock interaction and evaporation and precipitation processes in caves. They are found commonly on Earth in a plethora of caves, including lava tubes. They are also commonly coated in biofilms or microbial mats on Earth, making them unique for studies in geobiology. Since lava tubes have been identified on the surface of Mars from remotely sensed images, there has been interest in studying Earth's lava tube systems as an analogue for understanding Martian subsurface environments. If cave mineral deposits were found on Mars, they could indicate past or present water-rock interaction in the Martian subsurface. Martian lava tubes could also provide insights into habitable subsurface environments as well as conditions favourable for the synthesis and preservation of biosignatures.

In this study, secondary mineralization in lava cave systems from Lava Beds National Monument, CA is examined. Speleothems have been observed growing on all surfaces of the caves, including cave ceilings, floors, walls and overhangs. The first part of this thesis seeks to understand the geochemistry of these secondary mineral systems, as well as determine their possible relation to the biofilms. The speleothems were analysed in relation to the larger environmental and geological context it was in, and this was achieved through isotopic, geochemical and microscopic analysis. The second section of this study focuses on microscale analysis of the mineral-organic relation of layers within the cross section of the individual speleothems. This section seeks to understand further the formation history as well as the detection of biosignatures and their relation to the cave minerals.

Résumé

Les spéléothèmes coralloïdes ou coraux de cavernes sont des gisements de minéraux secondaires qui ressemblent à la forme d'un corail et se développent par infiltration des eaux souterraines, interaction eau-roche et processus d'évaporation et de précipitation dans les grottes. On les trouve couramment sur Terre dans une pléthore de grottes, y compris des tubes de lave. Ils sont également généralement recouverts de biofilms ou de nattes microbiennes sur Terre, ce qui les rend uniques pour les études en géobiologie. Depuis que des tubes de lave ont été identifiés à la surface de Mars à partir d'images de télédétection, l'intérêt d'étudier les systèmes de tubes de lave de la Terre en tant qu'analogue pour la compréhension des environnements souterrains martiens. Si des gisements de minéraux souterrains étaient découverts sur Mars, ils pourraient indiquer une interaction passée ou actuelle entre l'eau et la roche dans le sous-sol martien. Les tubes de lave martiens pourraient également fournir des informations sur les environnements souterrains habitables ainsi que sur les conditions favorables à la synthèse et à la conservation des biosignatures.

Dans cette étude, la minéralisation secondaire dans les systèmes de grottes de lave du monument national de Lava Beds, en Californie, est examinée. Des spéléothèmes ont été observés sur toutes les surfaces des grottes, y compris les plafonds, les sols, les murs et les surplombs. La première partie de cette thèse cherche à comprendre la géochimie de ces systèmes minéraux secondaires, ainsi qu'à déterminer leur relation possible avec les biofilms. Les spéléothèmes ont été analysés par rapport au contexte environnemental et géologique plus large dans lequel ils se trouvaient, grâce à une analyse isotopique, géochimique et microscopique. La deuxième partie de cette étude porte sur l'analyse à l'échelle microscopique de la relation

minéral-organique des couches dans la section transversale des spéléothèmes individuels. Cette section cherche à mieux comprendre l'histoire de la formation ainsi que la détection des biosignatures et leur relation avec les minéraux des grottes.

Preface

This study is conducted as a part of the Astrobiology Training in Lava Tubes (ATiLT) project funded by the Canadian Space Agency's *Flights and Fieldwork for the Advancement of Science and Technology* (FAST) program. The objectives of ATiLT are to: 1. Investigate remote detection and characterization of subsurface lava tubes by geophysical methods, 2. Investigate secondary minerals as records of paleoenvironmental information and biosignatures in lava tubes, and 3. Investigate cryomicrobiology of ice-rock interface in lava tubes. The field site for this project in anticipation of answering these questions was chosen to be Lava Beds National Monument in Northeastern California. The field work within the park is allowed under the NPS permit: LABE-2016-SCI-0011. Initial field analysis and site surveying was done in November 2016, followed by field work in May-June 2017 and April-May 2018. The submission of this thesis is to fill the project objectives of investigating secondary minerals within lava tubes for paleoenvironmental and/or biosignature indicators. Specifically, this project will look at coralloid speleothems and their relation to the biofilms that are present in the caves.

This thesis contains two manuscripts, and the author is the main contributor of both sections, with co-supervisors, Richard Léveillé and Peter Douglas being co-authors. The first manuscript will be an overview of the project and will be titled *Speleothems as a record of geochemical and biological processes in basaltic lava tubes in Northern California for a planetary analogue*. The second section will be shorter and will be more focused on the spatial analysis within a speleothem and will be titled *Spatial analysis of the mineral and organic components of a speleothem in basaltic lava tubes.* All co-authors have contributed or provided guidance in the analysis and/or interpretation of the data.

Acknowledgements

There are a lot of people to thank for the submission of this thesis. First and foremost, I need to thank my supervisors Dr. Richard Léveillé and Dr. Peter Douglas. There have been so many times I can recall when I felt lost and discouraged during my research, and they have been a constant source of encouragement and guidance. Thank you to Richard for starting this whole project with me and giving me so many opportunities to learn and conduct my own research. I have been lucky enough to be given so many opportunities to travel and look at planetary analogues not just from the perspective of this project but in terms of other geological environments. I would also like to thank Peter who took on the role of my being my supervisor when I arrived at McGill University. He has welcomed me into his lab group and has dedicated a lot of his time discussing and encouraging me throughout my master's degree.

This project would not have been possible or as enjoyable without the ATiLT team. Brady O'Connor, who was a great field assistant during my second field season and provided great discussions throughout my Master's. Pablo Sobron, thank you for always being so positive whenever we meet, whether it's in the field or at conferences. I would like to also thank Christopher Brown and Skyler Mallozzi who along with Brady explored all the different lava tubes with me during our field season together. In addition, I would also like to thank the rest of the field team, Christopher Patterson, Joshua Ford, Claire Samson and Michael Cunningham. I would also like to thank the park rangers at Lava Beds NM, Randall Paylor and David Riggs, who have been instrumental in guiding us in our field research.

There were also crucial parts of my thesis that couldn't have been done without the help of Michael Daly and his students, Cosette Gilmour and Catheryn Ryan. Thank you for allowing me to join your lab for my brief visits and making me feel like a part of the team.

There are also several members of the department whom I must thank for giving me advice and helping me with either research resources, laboratory space, equipment support or providing me with discussions in my research: Jeanne Paquette, John Stix, Don Baker, Galen Halverson, Lang Shi, Anna Jung and Isabelle Richer. I would like to show my appreciation to Redpath Museum, in particular Peter Tarassoff and Anthony Howell, for aiding me in finding appropriate minerals for comparison in the Raman analysis. I would also like to thank Olivier Sulpis, Monika Rusiecka and Rebecca Paisley who have helped me with lab work and/or instrument training. I would like to thank Kelsey Lamothe for helping me edit numerous conference abstracts, scholarship applications and poster presentations. I appreciate how much time they have all taken out of their schedule to help me with my thesis.

To all the friends I've made during my Master's: Rowan Wollenberg, Rebecca Paisley, Victoria Tweedie, Lauren Somers, Clara Waelkens, Monika Rusiecka, Kelsey Lamothe, Caroline Seyler, Olivier Sulpis, Wilder Greenman, Kyle Henderson and more, you guys have kept me sane with pub trivia nights, movie nights, hikes, karaoke and craft days. I have had a much better experience living in Montreal because of all of you. I would like to thank Rowan Wollenberg and Becky Paisley for helping me navigate being a graduate student and for always being there to motivate me with school work as well as real life. Thank you to Flavio Peter Weinstein Silva for pushing me and encouraging me endlessly, I would be a lot more stressed without your constant support. Lastly, I would like to thank my parents and my brother, John Ni, for being supportive of my studies.

Table of Contents

List of Figures

List of Tables

Preface to Chapter 1

Background knowledge on the subject of this thesis is summarised in the following literature review section. This was completed to analyse the state of research on related topics for this thesis. Relevant sections from this chapter will be repeated in the background sections of Chapter 2 and 3.

1: Introduction and Literature Review

1.1 Lava tubes and the Medicine Lake Volcano

1.1.1 Lava Tubes

Lava tubes are caves that generally form when lava flows downhill; the outer layer cools and crystallizes first, leaving the hotter inner core to continue flowing, creating a void space which eventually leaves behind a cave. They are commonly formed in pahoehoe flows at low effusion rates, but have also been described in a'a lava flows (Calvari and Pinkerton, 1999). Lava tubes are frequently found in volcanic settings all around the world including at Mount Etna, the Hawaiian islands, Jeju Island, Easter Island, Canary Islands, the Azores and many more locations (Peterson et al., 1994; Calvari and Pinkerton, 1999; Woo et al., 2008; Northup et al., 2011; Miller et al., 2014). Furthermore, they are even thought to play a significant role in producing basaltic shield volcano morphology due to their role in transporting lava to locations far from the source (Peterson et al., 1994).

Since lava tubes are formed due to volcanic activity, they are often complex in morphology and result in cross-cutting relationships through time. Lava tube cave systems are commonly observed to have stacked flows, complicated branching systems and come in various sizes and shapes. Due to the nature of lava flows, there are some primary geological features and structures that are unique to lava tube caves. Some of these indicate the magmatic history, such as flow lines and step marks which show the flow direction of the lava at the time of cooling. Other features such as lavacicles, or lava stalactites and stalagmites, are formed as active lava

drips from the ceiling of the cave and cools. Lavacicles are formed on a much faster time scale, in the time of cooling magma, and play a significant role in concentrating areas for secondary mineral deposition. The primary host rock mineralogy and geochemistry potentially plays a huge role in secondary mineralization (Woo, 2005).

There are also some larger scale considerations regarding lava tube cave systems. Due to stacked flows and collapsed sections, a complex air flow system is expected in the caves. A change in seasons will also affect how the air flows in the caves. When the temperature outside of the caves is cold, it will sink into the subsurface, displace the warm air out and trap the cold air in. When the temperatures outside shift to be warmer, cold air will continue to be trapped in the cave, allowing for stable temperatures year-round (Williams et al., 2010). An example of this is seen in lava tubes with sections of cold traps, allowing for perennial ice (Racovita and Onac, 2000; Perşoiu and Pazdur, 2011). In large lava cave systems with many openings to the surface and levels on which air can travel, the slightest shift in circulation can affect the subsurface conditions (De Freitas et al., 1982; Perry, 2013). This is important as it can shift hydrological, biological and geological processes within the lava tube (De Freitas et al., 1982; Yonge and MacDonald, 1999; Perry, 2013).

1.1.2 Site Context

This following section on site context is a summary of the relevant sections pertaining to Lava Beds National Monument from the USGS report of Medicine Lake volcano, and as such the geological information in these sections are credited to the report unless otherwise stated (Donnelly-Nolan, 2010). The convention of the volcanic units written in this section, that is three

lower-case letters, corresponds to the convention set by the USGS report that accompanies the geologic map of the area.

Lava Beds National Monument (LBNM) is a designated park located on the Northeastern flank of the Medicine Lake volcano (MLV). MLV lies in a tectonically active zone behind the volcanic front of the Cascades arc in the Basin and Range tectonic province and is estimated to have been active starting 500 000 years ago based on K-Ar and $^{40}Ar/^{39}Ar$ argon dating (Donnelly-Nolan and Lanphere, 2005). The eruptive history of the region can be separated into five constrained stages: 1) early history from 500 ka to 300 ka, 2) 300 ka to 180 ka, which includes the stratigraphic marker of dacite tuff (see below), 3) 180 ka to 100 ka, 4) 100 ka to 13 ka, and 5) postglacial eruptions less than 13 ka.

During the first eruptive stage, Medicine Lake volcano was dominated by the eruption of silicic domes and flows with the oldest successfully dated lava being a rhyolite dome which has a $^{40}Ar/^{39}Ar$ age of 475 ± 29 ka. During the second eruptive stage, beginning around 300 ka, mafic lavas dominated MLV, with the appearance of more than half of the isolated cinder cones observed in the region. At the end of this eruptive stage is the eruption of the dacite tuff of Antelope Well which was widespread and the only known ash-flow tuff, becoming a stratigraphic marker bed for MLV. The third eruptive stage, from 180 to 100 ka, is the second most frequent period of eruption of the volcano and is dominated by basalt and basaltic andesite units. There were also units of andesite erupted during this period, accounting for half of the andesite units found at MLV.

Eruptive stages four and five are the stages that dominate the Lava Beds National Monument area, occurring from 100 to 13 ka and from 13 ka to the present, respectively. The fourth eruptive stage saw fewer eruptions during the 85 000 year period than the third eruptive

stage, with the eruptions occurred mainly on the eastern flank of the volcano. The basalt of Mammoth Crater (bmc) which hosts most of the lava tubes in LBNM (and this study) erupted during this time with a $^{40}Ar/^{39}Ar$ age of 36 ± 16 ka. This unit is made up of compositionally variable basalt and basaltic andesite with a silica content ranging from 48.4-55.9%. The bmc covers roughly 250 km^2, with a volume estimated to be at least 5 km^3. This unit is made up of numerous flows from several different vents, including Mammoth Crater, Modoc Crater, Bearpaw Butte, and Bat Butte. Areas near the vents are where the measured silica content is the highest. The facies of this unit is described as fine-grained and glassy, containing plagioclase phenocrysts in a groundmass of plagioclase, microlite, clinopyroxene and olivine in a glassy matrix (Donnelly-Nolan and Champion, 1987). The bmc contains the Skull Ice Cave chain as well as the caves located in the Cave Loop. Also in the fourth eruptive stage is the basalt of Caldwell ice (bci). The bci has been described as an aphyric basalt, with a high silica content of 52.8%. The flow for this system was supplied from a source south of the Caldwell Butte. Most of this unit is buried by the basalt of Valentine cave (bvc). The basalt in this unit is described as fine-grained, with intersertal to diktytaxitic texture with plagioclase crystals sitting in a groundmass of olivine, plagioclase and clinopyroxene (Donnelly-Nolan and Champion, 1987).

The fifth eruptive stage is classified as the postglacial eruptions after the retreat of the Pleistocene glaciers, roughly 13 ka to the present. There have been 17 eruption events in this age so far and they are scattered widely across the volcano. The silica composition is broad, ranging from 47.2% to 74.6%, with a gap between 58.1% to 63.3%. The eruptions during this stage were episodic, with eight of the events occurring about 12.5 ka (Nathenson et al., 2007). In the late Holocene mafic and silicic eruptions both occurred, but silicic eruptions were more frequent. The basalt of Valentine cave (bvc), is a unit that hosts lava tubes from this last eruptive stage. This

basalt unit is described as sparsely porphyritic basalt and basalt andesite, having an average silica content of 53.0%. It is considered an early flow in this stage, with a radiocarbon age, calibrated with paleomagnetic direction, of 12 260 years B.P. It erupted in a northwest-trending linear array of spatter cones just south of the park limits. It is unusual for flow with such high silica content to generate lava tubes, but it is thought that it may be related to the high titanium and iron contents of the lava. This system includes one of the park's most popular sites – Valentine Cave.

To complete the geologic history of the area, it is also important to discuss the glacial history. There is definitive evidence of transportation and deposition of glacial till in the MLV region (Anderson, 1941). There is also evidence of glacial striations on the rim of the caldera. In some areas of MLV, glacial till covers large enough regions to obscure underlying units. The area is interpreted as not being heavily impacted by glacial activity due to the lack of U-shaped valleys or major topographic changes. There are only small volumes of glacial till, with a few small cirques seen and minor removal of lava rock surfaces. There is evidence indicating at least two periods of glaciation, with different ice limits from different time periods. It is also believed that ice moved away from the caldera as well as accumulated within it.

1.2 Speleothems and other secondary mineral deposits

Speleothems are secondary mineral deposits formed in caves as minerals precipitate from cave water. Speleothems are distinguished from sediments accumulated in the cave, which are not growing directly in the cave, are not consolidated, or do not contain a structure. Speleothems are also separate from the primary host rock, which in a lava tube is the igneous rock formed

from the initial lava flow. The term speleothem refers to the actual growth structure and morphology of the deposit, such as coralloid speleothem, stalactite, stalagmite, cave bacon, etc. In karst caves, the type of speleothem formed is seen to be dictated by a number of variables, including substrate on which the deposit forms, water supply, aerosols, rate of degassing and evaporation (Caddeo et al., 2015; Vanghi et al., 2017).

Coralloid speleothems are speleothem structures that resemble the shape of coral. Coralloid speleothems have been found forming on ceilings as well as the floor of lava tubes (Woo et al., 2008). Although coralloid formation has not been studied extensively in lava tubes, in limestone caves the location of their formation is thought to be related to the texture and structure of the substrate, water supply, degassing and evaporation (Hill and Forti, 1997; Caddeo et al., 2015; Vanghi et al., 2017). Coralloid speleothems have even been found growing on bones and debris on the ground of caves through hydroaerosols, which form when cave drips fragment (Vanghi et al., 2017). On Jeju Island, coralloid speleothems composed of mainly calcite, aragonite, and opaline silica have varying morphologies thought to be due to the original precipitation of calcite and aragonite with differences in structure due to later replacement by the silica (Woo et al., 2008).

1.2.1 Relation of carbonates and amorphous silica

Both carbonate minerals and amorphous silica are found widely within caves. There are many factors that determine carbonate or silica precipitation in systems that contain both mineral species. The pH variations and the chemical composition of cave waters are thought to be the controlling factors for precipitation of carbonates and opal in caves (Hill and Forti, 1997). Since speleothems form from water-rock interaction with the host rock, they are expected to be similar

in chemical composition to the cave water and the surrounding basalt (Woo, 2005). Even within carbonates, the precipitation of aragonite or calcite are influenced by factors in the cave such as pH, Mg/Ca ratio in the cave waters and evaporation rates (Woo et al., 2008).

1.3 Biosignatures

A biosignature is any substance that provides scientific evidence of past or present life. Biosignatures are not only defined by the probability of life creating the signature but also by the improbability of abiotic processes producing it (Abrevaya et al., 2016). This signature can be:

1. physical and textural, as in the case with fossils or trace fossils;

2. molecular, signatures detected through molecular compounds such as phospholipid fatty acids or nucleic acids;

3. isotopic, fractionation influenced through biological processes, or;

4. morphologic, seen in structures or characteristics that are distinct to biogenic minerals.

We see preservation of all these signatures of life on Earth, and in our understanding of life, aim to apply these same requirements for possible life outside of our planet. As with the case on Earth, any one of the signatures might not indicate life and, in general, it is good practice to verify the presence of more than one type of biosignature, as such identifying biosignature suites. Since there has been a constant fascination in the scientific community about identifying past life on our planet, and outside of it, it has led to a lot of debate about what qualifies as a definitive signal that life exists or existed. In this search, there have also been lessons learned on the importance of rigorous lab technique and preparation. There has also been constant debate on

signals of the origin of life on Earth in trying to connect primitive structures to the life that is known today. This leads to further questions of if life on Earth is truly representative of life as a whole and if we can use this definition for identifying life outside of Earth (Abrevaya et al., 2016).

1.3.1 Isotope Systems

Isotopes have been useful in a variety of contexts for studying Earth processes, including tracing pollutants, determining origin sources, geologic dating, and tracing biogeochemical cycling. In a cave environment, some of the most important and widely studied isotopes are δD and $\delta^{18}O$ for cave water and $\delta^{13}C$ for carbonates. In analysis of organic matter, stable isotopes of carbon, nitrogen and sulphur are commonly analyzed.

1.3.1.1 Isotopes for analysis of water:

The hydrologic cycle is widely studied for management of water resources, pollution and understanding earth processes. It is a global cycle that circulates water around our planet, allowing for life to occur, temperatures to be regulated and many geological processes to transpire. It can be studied on a global and regional scale, and natural terrestrial water that is constantly cycled is expected to fall on the global meteoric water line in terms of H and O isotopes (GMWL). For a basaltic cave, meteoric water percolates through the host rock, with the water interacting with minerals within the basalt until it reaches the cave where evaporation and degassing processes occur and allow for minerals to precipitate. This process is thought to take place in a relatively short time period so that the cave drip water should have an isotopic water value reflective of the GMWL. In Northeastern California, the average isotopic composition for meteoric water is -11.0 ‰ and -70.5 ‰, for $\delta^{18}O$ and δD, respectively (Ingraham and Taylor,

1991). Since living things uptake water, isotopes of water can indicate source and provide time information. $\delta^{18}O$ and δD can also be recorded in speleothems than form under the influence of evaporation processes, by analyzing the minerals that are present.

1.3.2 Textural and Physical Biosignatures

Physical and textural biosignatures such as microfossils and stromatolites indicate much about past life on Earth. Not only do they indicate the presence of life, they can be used to infer behaviours, life evolution, depositional environments and past atmospheric conditions. On Earth, the sedimentary rock record extends back billions of years, in some cases preserving the fundamental events that lead to life seen today. Fossils on Earth show the biological history of the planet from the extinction of dinosaurs, to the first emergence of plants. Focusing on its earliest record of microbial evolution, ~3800 - 1800 Ma (Knoll et al., 2016), there have been many debates on viable physical biosignatures. Stromatolites, which are seen in the rock record as laminated structures and can be domal or conoidal, are some of the most widely accepted paleobiological markers both in terms of geological coverage and geological time. They are a great indicator in terms of biosignatures because they exist widely today and provide a modern analogue to understand ancient processes. Based on living stromatolites today, stromatolites appear to grow and accrete as dense cyanobacterial mats through extracellular polymeric substance (EPS) trapping fine grained material which allows for carbonate precipitation (Reid et al., 2000). These processes and the relation of the abiotic sediment in relation to the biotic stromatolite can be seen in juxtaposition in these modern environments. In slightly younger stromatolites (~2 Ga), we see evidence of these biotic processes in textural features, but in older stromatolites, such as the ones in the Strelley Pool Formation, these textural biosignatures are not as well preserved (Knoll et al., 2016).

Behaviours of life can also be reflected in textural or morphological biosignatures, such as trace fossils which can be tracks, burrows, or feeding marks. There are heavily debated morphological features on Earth in terms of biotic versus abiotic processes. This includes the tubular structures found in pillow basalts of the Barberton Greenstone Belt from 3.4-3.5 Ga, or the filamentous features of the Apex chert in Western Australia from ~3.5 Ga (Schopf, 1993; Banerjee et al., 2006; Fliegel et al., 2010). If proven true, some of these morphological features could be the earliest evidence of life on this planet. However, in later research of the Apex chert, it has been argued that these simple morphological features could be formed just as easily through abiotic processes (Brasier et al., 2005). This shows the importance of finding complementary biosignatures, especially for planetary analogues, as less is understood about the geological context of the rocks in which the biosignature is in.

1.4 Martian Analogues

There are many geological sites on Earth that have been studied over the last century for their similarity to Mars. These range from modern analogues, to ancient analogues for the origin of life on Earth. Since as early as the mid-20th-century, our own planet has been recognized as being a good model for extraterrestrial knowledge (Urey, 1952; Léveillé, 2010). The benefit to understanding more about Earth processes to apply to other planetary or lunar bodies is that it will help make comparisons and look at the solar system holistically. Additionally, it is much easier and resource efficient to try and understand as much as possible about the same system on Earth. Another benefit is that more methods and more thorough analysis can be tested on Earth to plan better for analysis on Mars (Rummel, 2005; Mulugeta et al., 2011). Doing analogue

studies provides a point of reference for any future data that may be collected from Mars (Boston et al., 2001; Cady et al., 2003).

Since the identification of lava tubes from orbital imagery on Mars, there has been interest in them as possible candidate sites for targets for future astrobiological research (Léveillé and Datta, 2010). The current surface conditions on Mars are very harsh and unfavourable to preserving biosignatures due to erosional processes, harsh radiation and extreme temperatures. On Earth, caves are unique ecosystems, with biology adapted for dark and sometimes cold environments. In favour of lava tubes being a target for astrobiology, life is ubiquitous in cave formations all over Earth, found in different types, ages and settings of caves (Jones, 2001; Northup and Lavoie, 2001; Léveillé et al., 2002; Hathaway et al., 2014; Tomczyk-Żak and Zielenkiewicz, 2016).

Lava tubes are commonly found in terrestrial basaltic volcanism on Earth and is expected to be the same on Mars. There are suspected lava tube series on Mars found in multiple volcanic regions including, Tharsis Montes (Grin et al., 1998; Cabrol et al., 2009; Cushing, 2012). They have been identified through sinuous and linear depressions and channels in volcanic settings (Wyrick et al., 2004; Cushing, 2012). In other cases, they have also been identified through the presence of skylights and pit chains (Cushing, 2012; Jung et al., 2016). In lava-tube formation, the length and diameter of the tube are related to properties such as gravity, regional topography, lava viscosity and effusion rates (Keszthelyi, 1995; Keszthelyi et al., 2006). Due to Mars' lower gravity, lava tubes are expected to be larger in comparison to lava tubes found on Earth. In addition, lava tubes in the dark smooth lava flows of Arsia Mons show flow inflation as evidence from steep sided, terraced margins, smooth plateaus and digitate breakout lobes (Crown and Ramsey, 2017). Lava flow inflation is seen on terrestrial analogues where there is uniform uplift

of entire flow sheets due to sustained lava injection allowing for increasing size of the flowing core. The lava inflation features seen in the tube-fed flows of Arsia Mons are much larger than the same inflation features seen in Hawaiian flow fields, suggesting another possibility for larger than expected lava tubes on Mars in comparison to Earth (Crown and Ramsey, 2017). Another effect from the lower gravity on Mars is that lava will have a slower flow rate, which will also lead to more heat loss per distance, which will result in shorter flows (Rowland et al., 2004).

Preface to Chapter 2

Speleothems, secondary mineral deposits within caves, are important geological samples of study from an astrobiology point of view. They form due to hydrologic processes on Earth and interact with the surrounding system as the deposit grows, recording information about its environment. Although speleothems are widely studied on Earth in limestone caves, there is less knowledge about them in basaltic caves, such as lava tubes. This chapter of the thesis will be focused on quantifying what these speleothems are composed of, what influences their formation and determining whether they record any biological signatures from the biofilm that is often seen covering them. As the field site for this study at Lava Beds National Monument has not been studied for these speleothems exclusively, this manuscript has been written to inventory the geochemical processes of the caves and its surroundings in relation to the speleothems. This will set a foundation for future research in the park and on lava tubes as a target for astrobiological analyses on other planetary or lunar bodies.

2: Speleothems as a record of geochemical and biological processes in basaltic lava tubes in Northern California for a planetary analogue

Jenny Ni[1], Richard Léveillé[1], and Peter Douglas[1]

[1] Department of Earth and Planetary Sciences, McGill University, Montréal, Québec

Key words: Biosignatures, speleothems, lava tubes, planetary analogue, Mars

2.1 Abstract

Speleothems are secondary mineral deposits that form due to groundwater seepage, water-rock interaction and evaporation and precipitation processes inside of caves. As such, they are important indicators of an environment, what is present in it and the processes that are occurring there. In this study, speleothems from basaltic lava tubes situated in Lava Beds National Monument, CA are observed growing adjacent to biofilms in the present day. The speleothems formed in these basaltic caves are predominantly made up of opal, with chalcedony, calcite and other minor minerals also detected through powder X-ray powder diffraction. This silica rich system is important in preserving physical and textural biosignatures of the biofilms that are on the speleothems. Carbon isotopes were also analysed from the carbonate minerals and organic carbon from aliquots of the same speleothem samples, as well as from DIC from cave waters, and other surrounding organics. The $\delta^{13}C$ of the carbonates in the speleothem are 13.2‰ enriched from the $\delta^{13}C$ of the DIC of the drip water in the caves. Results show around a 27.6‰

difference in the inorganic and organic carbon components of the speleothem. Samples of overlying soil and plant matter have $\delta^{13}C_{org}$ of -24.9‰ and -27.9‰, respectively; it is proposed that the source of carbon in the organic component of the speleothem is from soil organic matter that has percolated through and is constantly recycled at the cave speleothem interface. In analysing the speleothems, we demonstrated the preservation of biological signatures in the speleothems in lava tubes.

2.2 Introduction:

Lava tubes are lava caves formed as lava flows downhill, with the outer part of the flow crystallizing first due to cooler temperatures of the air and surrounding rock and the inner hotter region continuing to flow downhill, draining the tube and leaving behind a cave. They can be complex systems, resulting in stacked and braided cave networks. They are widely found in basaltic volcanic environments on Earth in Korea, Iceland, Australia, Hawaii, Azores and Canary Islands. In the continental USA, at Lava Beds National Monument (LBNM) in Northern California there are over 800 known lava tubes. These caves are on the Northeastern flank of the Medicine Lake Volcano (MLV), an area with an estimated eruptive history beginning around 500 ka (Donnelly-Nolan et al., 2008).

Speleothems are structures formed in caves by the precipitation and deposition of minerals from the evaporation and degassing of cave water. As speleothems are secondary mineral deposits, they show similar mineralogy and chemistry to the host rock, which in this case is the basaltic lava tube. There are various types of speleothems found in the lava tubes located within LBNM, with coralloid speleothems being the most abundant. Soda straws, which are

tubular stalactites, and flowstones, which are sheet-like deposits that form on walls or floors, also occur. Coralloid speleothems are speleothem structures that resemble the shape and morphology of marine corals. Coralloid speleothems have been found forming on ceilings as well as the floor of lava tubes within the park. Although coralloid formation has not been studied extensively in lava tubes, in limestone caves their formation and morphology is thought to be related to the texture and structure of the substrate, water supply, degassing and evaporation (Hill and Forti, 1997; Caddeo et al., 2015; Vanghi et al., 2017).

If life existed on Mars in the past, it is thought that it is most likely to be microbial. Microbial life is the most diverse life on Earth, with microbial species existing in almost every niche on this planet, even surviving at extreme pH, temperatures and salinities (Raes, 2010; Thompson et al., 2017). The fact that they are widespread and diverse is also a positive point for studying them for astrobiology targets. In the present day, biofilms and microbial mats are observed growing adjacent to the speleothems in many of the lava caves within the park and worldwide (Léveillé et al., 2007; Hathaway et al., 2014; Miller et al., 2014; Riquelme et al., 2015; Lavoie et al., 2017). They are seen coating the surfaces and growing in cracks of speleothems as well as on basalt and cave sediment surfaces. In the caves, there will be a lack of photosynthesis leading to absence of primary production of organic matter from plants, resulting in resource limiting environments (Northup and Lavoie, 2001). It is seen that there are species who have adapted to the dark, limiting environment, with microbial species found within caves that are vastly different from what is found in the overlying soil (Lavoie et al., 2017).

2.3 Site and geologic history:

Lava Beds National Monument is in a semi-arid desert environment with an altitude ranging from 4000 to 5700 feet. It is situated in the geologic region of the Modoc Plateau in Northern California. It has warm and dry summers averaging highs of 25°C and cold snowy winters averaging lows of -3°C. The common vegetation cover in the park include bunchgrasses, sagebrushes, junipers and ponderosa pines, although some flows in the park have little vegetation cover and are still mostly barren volcanic flows (DiPaolo et al., 2015).

2.3.1 Geologic history

This following section on site context is a summary of the relevant sections pertaining to Lava Beds National Monument from the USGS report of Medicine Lake volcano, and as such the geological information in this section and section 2.3.2 are credited to the report unless otherwise stated (Donnelly-Nolan, 2010). The convention of the volcanic units written in this section, that is three lower-case letters, corresponds to the map units and convention set by the USGS report that accompanies the geologic map of the area.

Lava Beds National Monument (LBNM) is a designated park located on the Northeastern flank of the Medicine Lake volcano (MLV). MLV lies in a tectonically active zone behind the volcanic front of the Cascades arc in the Basin and Range tectonic province and is estimated to have been active starting 500 000 years ago based on K-Ar and $^{40}Ar/^{39}Ar$ argon dating (Donnelly-Nolan and Lanphere, 2005). The eruptive history of the region can be separated into five constrained stages: 1) early history from 500 ka to 300 ka, 2) 300 ka to 180 ka, which includes the stratigraphic marker of dacite tuff (see below), 3) 180 ka to 100 ka, 4) 100 ka to 13 ka, and 5) postglacial eruptions less than 13 ka. The first three eruptive stages do not host any

lava tubes in the site or this study and will not be discussed, but they are described in Donnelly-Nolan, (2010).

The fourth eruptive stage saw fewer eruptions during the 85 000 year period than the third eruptive stage, with the eruptions occurred mainly on the eastern flank of the volcano. The basalt of Mammoth Crater (bmc) which hosts most of the lava tubes in LBNM (and this study) erupted during this time with a $^{40}Ar/^{39}Ar$ age of 36 ± 16 ka. This unit is made up of compositionally variable basalt and basaltic andesite with a silica content ranging from 48.4-55.9%. The bmc covers roughly 250 km^2, with a volume estimated to be at least 5 km^3. This unit is made up of numerous flows from several different vents, including Mammoth Crater, Modoc Crater, Bearpaw Butte, and Bat Butte. Areas near the vents are where the measured silica content is the highest. The facies of this unit is described as fine-grained and glassy, containing plagioclase phenocrysts in a groundmass of plagioclase, microlite, clinopyroxene and olivine in a glassy matrix (Donnelly-Nolan and Champion, 1987). The bmc contains the Skull Ice Cave chain as well as the caves located in the Cave Loop. Also in the fourth eruptive stage is the basalt of Caldwell ice (bci). The bci has been described as an aphyric basalt, with a high silica content of 52.8%. The flow for this system was supplied from a source south of the Caldwell Butte. Most of this unit is buried by the basalt of Valentine cave (bvc). The basalt in this unit is described as fine-grained, with intersertal to diktytaxitic texture with plagioclase crystals sitting in a groundmass of olivine, plagioclase and clinopyroxene (Donnelly-Nolan and Champion, 1987).

The fifth eruptive stage is classified as the postglacial eruptions after the retreat of the Pleistocene glaciers, roughly 13 ka to the present. There have been 17 eruption events in this age so far and they are scattered widely across the volcano. The silica composition is broad, ranging from 47.2% to 74.6%, with a gap between 58.1% to 63.3%. The eruptions during this stage were

episodic, with eight of the events occurring about 12.5 ka (Nathenson et al., 2007). In the late Holocene mafic and silicic eruptions both occurred, but silicic eruptions were more frequent. The basalt of Valentine cave (bvc), is a unit that hosts lava tubes from this last eruptive stage. This basalt unit is described as sparsely porphyritic basalt and basalt andesite, having an average silica content of 53.0%. It is considered an early flow in this stage, with a radiocarbon age, calibrated with paleomagnetic direction, of 12 260 years B.P. It erupted in a northwest-trending linear array of spatter cones just south of the park limits. It is unusual for flow with such high silica content to generate lava tubes, but it is thought that it may be related to the high titanium and iron contents of the lava. This system includes one of the park's most popular sites – Valentine Cave. Another important feature of the park is the pumice layer that covers LBNM which was deposited around 900 years ago from the eruption of the nearby Glass Mountain, which is also the last eruption in the MLV region (Waters et al., 1990; Donnelly-Nolan, 2010).

2.3.2 Caves for this Study

As mentioned in section 2.3.1, the caves that have been sampled in this study are from volcanic units from the fourth and fifth eruptive stages: bci, bmc, and bvc. There were 12 total caves sampled across these three different units. The caves were selected based on presence and abundance of speleothems, presence of biofilms, and wetness of cave. Caves with less human traffic were also preferred to get as pristine samples as possible. The 12 caves were sampled for broader understanding of the geochemical trends of the cave water and mineralogy of speleothems in the park. The relation of the 12 caves to the geological units is summarized below in Table 1. Of the 12 caves sampled, 10 contained coralloid speleothems, and 4 contained perennial ice. Coralloid speleothems and perennial ice were not often found in the same caves; only in one cave were they observed adjacent, and in one other cave they were found in

completely separate rooms of the same cave. Since this study is focused on coralloid speleothems, caves with speleothem growth were prioritized, but caves with perennial ice were sampled for water. All 10 of the caves that contained speleothems were sampled for speleothem samples, and water and/or soil samples if present. Two caves, YEL and CRF, were further studied for more detailed isotopic, mineralogic, and physical analyses due to the rich abundance of speleothems in the caves.

CRF cave located in the basalt of caldwell ice is a narrow and small cave in comparison to other lava tubes in the park. Passages explored within the lava tube range from around 0.5-4 metres in height and are often 1-2 metres across. The cave contains common features observed in other caves in the park, including lavacicles, coralloid speleothems, soda straws, biofilms, inwashed pumice heaps, and primary lava flow features. This cave shows complexity as there are two main passages that branch off continuing down the main passage, with one splitting down trending east and the other passage trending northeast. There is a slope leading in from the entrance of the cave showing mud, surface debris, moss and pumice inwashing into the cave. Upon the first survey in November of 2016, the cave was noted to be very wet and muddy, and was also the case in June of 2017; however, in May of 2018 the cave was noticeably drier. Speleothems were sampled from the main passage of the cave as well as the two smaller sub-passages. Coralloid speleothem samples collected from the ground were larger and more globular than observed in other caves ranging from a few millimetres to around 4 centimetres.

YEL cave is located in the bmc, which is the basalt flow hosting the majority of lava tubes within LBNM. From the entrance of the cave, it immediately splits off into two passages, one trending northeast and one trending west which will subsequently be referred to as the left and right passage, respectively. Similar to CRF, the cave is also quite narrow, especially

proceeding down the right passage which ranges from 0.7-3 metres. There are lava pillars, lavacicles, rafted breakdown and very prominent lava flow lines observed in this passage. As well, there is widespread mud present on the floor of the cave. Biofilms are observed to be not only coating the speleothems, but also the mud on the floor. In the left passage of YEL cave, a noticeable additional primary feature is the presence of lava falls where magma has flowed down from the top layer to the next, and because of this the passage is less narrow than the right passage, ranging from 1-5 metres.

2.4 Methods:

2.4.1 Sampling:

Water samples were collected across all three field seasons in November 2016, May-June 2017 and April-May 2018. In the first field season, a small set of samples was collected to identify general trends in water chemistry in LBNM, so major ions and stable isotopes were analyzed. That sampling was expanded during the second field season with more samples from additional caves. In the last field season, drip rate was measured on site and dissolved inorganic carbon (DIC) concentration and $\delta^{13}C$ were measured later in the laboratory. Temperature and pH readings were taken with a multimeter in the field during the time of sampling for every sample collected. Samples intended for DIC analysis were filtered with sterile 0.22 µm syringe filters. Samples were stored in 15 mL glass vials and transported in the dark and at low temperatures (around 4°C) to limit biological activity.

Speleothem samples were carefully collected during the field seasons in 2017 and 2018. Samples from caves with visually different morphologies and colours observed in the field were

catalogued and sampled. In addition, speleothems growing in different parts of the cave were sampled (ie. ground versus ceiling). Samples were taken from inconspicuous spots not at eye level, in keeping with LBNM policy. For bulk analysis of mineralogy, samples were selected based on the presence of a wide range of colours and textures, whereas samples with complete structures were selected for spatial analysis and microscopy. Several samples were also selected for analysis by SEM to analyse the surface of the speleothems.

Cave mud was sampled carefully with a scoopula from the cave floors. All samples were taken from inconspicuous spots. All cave mud was collected in areas that were wet, and in some cases, biofilms were seen coating the mud surface. Overlying soil from above the caves was also sampled with a scoopula. Overlying plant matter, specifically sagebrush leaves, due to it's widespread presence in the park, was sampled and collected in Whirl-Pak sampling bags. All cave mud, overlying soil and plant samples were prepared for isotopic analysis by freeze drying, followed by powdering using the mortar and pestle.

2.4.2 Isotopic Methods:

All isotopic analyses were performed at the Geotop Research Centre at Université du Québec à Montréal. The isotopes analyzed were δD_{water}, $\delta^{18}O_{water}$, $\delta^{18}O_{carb,}$ $\delta^{13}C_{carb}$, $\delta^{13}C_{DIC}$, $\delta^{13}C_{org}$, and $\delta^{15}N_{org}$. Cave drip and pool water samples were collected and filtered on site. Pool waters were collected using syringes and are defined as any pond of water on the cave floor, cave ice or cave mud. δD_{water}, $\delta^{18}O_{water}$ and $\delta^{13}C_{DIC}$, were analyzed from these samples. δD_{water}, and $\delta^{18}O_{water}$ were analyzed using a Los Gatos Research, Triple Liquid Water Isotope Analyser model T-LWIA-45-EP. The analysis was referenced to VSMOW-SLAP. For the $\delta^{13}C_{DIC,}$

alkalinity was measured using a digital TTT85 Titrator with an ABU80 Autoburette. DIC $\delta^{13}C$ was measured using an Isoprime 100 in CF mode with MicroGas. Measurements for $\delta^{18}O_{carb,}$ $\delta^{13}C_{carb}$, $\delta^{13}C_{org}$, and $\delta^{15}N_{org}$ were analyzed on aliquots of the same speleothem samples. Measurements for $\delta^{13}C_{org}$ and $\delta^{15}N_{org}$ were also analysed for soil and plant samples collected above and within the caves. Speleothem samples were powdered to be homogeneous on the sub-milligram scale and the organic fraction was run on an Isoprime 100 coupled in CF mode with Elementar Vario MicroCube. Organic carbon samples were treated with 12N HCl acid to fumigate for 24 hours to remove inorganic carbon prior to isotope analysis. The inorganic C was run on an Isoprime DI Multicarb and Isoprime 100 in continuous flow mode with MicroGas. The reference standards used were VSMOW for $\delta^{2}H$ and $\delta^{18}O$, VPDB for $\delta^{13}C$ and AIR for $\delta^{15}N$.

2.4.3 Geochemistry of Cave Water:

The cave drip and pool water samples were also analyzed for major ions using a Thermo Scientific iCAP 6000 Series ICP Spectrometer. A survey scan was originally conducted for common elements, and later quantitative runs were performed with standard curves created with elements of interest.

2.4.4 Mineralogy of Cave Speleothems:

Power X-ray diffraction with a Rigaku SmartLab was used to quantify the bulk mineralogy of samples. Samples of speleothem were powdered first using a mortar and pestle, and then bleached with 3% hydrogen peroxide and sonicated for 1-2 days until they stopped reacting and left to dry. The dried samples were then sieved through 45 µm spacing. The powdered samples were then loaded separately in a 10-disk automated sample changer containing circular sample dishes, with the discs rotating during analysis for further random

orientation in the measurement. The samples were analyzed from 2°-70° at a step rate of 0.01° in continuous mode.

2.4.5 Microscopy

A survey of mineralogy was performed using thin sections with a petrographic microscope. Analysis was also performed using a Hitachi SU5000 scanning electron microscope (SEM), to observe surface microbial features as well as speleothem cross-sections. Samples were uncoated, and samples selected for observing the surface were held by specimen mounts.

2.5 Results:

Within LBNM, 11 caves were sampled within the scope of this project, summarized in Table 1, listed from youngest to oldest flow. The bolded cave names are the caves where further geochemical, isotopic and mineralogic work was conducted on the speleothems.

Table 1: Summary of caves sampled in this project relating to their flow, ages and composition data of flow obtained from (Donnelly-Nolan, 2010). *Some caves are confidential due to park access and are therefore described using a random combination of letters. Superscript on cave names indicate what samples were taken there: c for mineral deposit samples, p for pool water samples, d for drip water samples and s for soil samples.*

Name of Flow	Composition of Flow	Age	Name of Cave
Basalt of Valentine Cave (bvc)	Sparsely porphyritic basalt and basaltic andesite. SiO_2: 53.0%	12.31 ka (radiocarbon, calibrated on basis of paleomagnetic direction)	VAL Cave ^{c}
Basalt of Caldwell Ice Caves (bci)	Aphyric basalt SiO_2: 52.8%	Late Pleistocene Underlies bvc flow	BIC Cave ^{c}
			CRF Cave ^{c,p,d,s}
			NIN Cave ^{c,p,d}
Basalt of Mammoth Crater (bmc)	Compositionally variable basalt and basaltic andesite. SiO_2: 48.4-55.9%	36 ± 16 ka ($^{40}Ar/^{39}Ar$)	COX Cave ^{p,d}
			GDO Cave ^{c,s}
			HPP Cave ^{c,p,d}
			HCC Cave ^{c,d}
			IWC Cave ^{c}
			MER Cave ^{p,d}
			SEN Cave ^{c,d}
			YEL Cave ^{c,p,d,s}

2.5.1 Morphology of coralloid speleothems

Speleothems collected for this study varied in size, morphology and colour. They were commonly found on cave floors, walls and ceilings where water seeps or pools were present. They were generally found in zones of complete darkness, and for the purposes of this study all samples collected were found in these zones. There were several morphological types of coralloid speleothem identified (Figure 1). Generally, speleothems found on the ground were thicker but shorter (average samples with length of 15-20 mm and width of 6 mm) than those from the ceiling (average samples with length of 25 mm and width of 3 mm). Although all were classified as coralloid speleothems, there are significant differences in the structure of the speleothems seen in LBNM. Some coralloid speleothems branch more, while others take the form of cylindrical stubs. There is also variation in the size of branches and clusters seen in the secondary minerals in the lava tubes. Structures collected from the ceiling and wall contained thinner branches in comparison to the stubbier branches from samples on the ground.

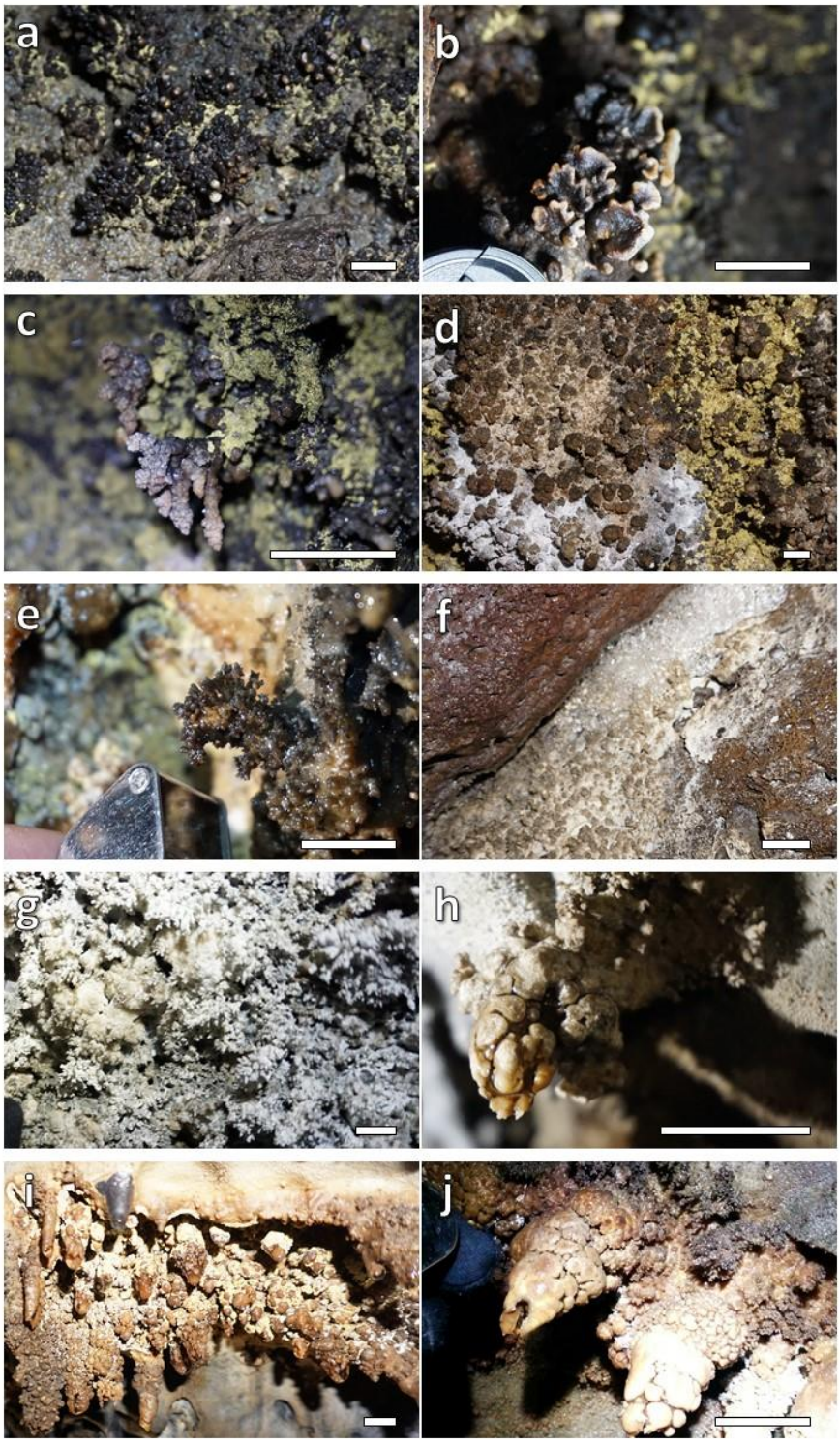

Figure 1 Different morphologies of coralloid speleothems sampled in LBNM. Scale bar in photos is approximately 2 cm. 1a,b are samples collected from the ground; yellow coloured biofilm is seen covering the speleothems, mainly occurring at the base. 1c,d,e are coralloid speleothems on the walls of the lava tube, showing different sizes of branching and clustering. 1d shows white, yellow, and tan biofilms covering the speleothems extensively. 1f shows coralloid speleothems on an overhang, with ice growing adjacent to the cluster of cave corals. 1g,h,i,j are some unique speleothems from the cave ceiling, in some cases as in 1i,j, it is seen that coralloid speleothems have formed on top of soda straw speleothems.

2.5.2 Mineralogy

Bulk mineralogy analysis by X-ray diffraction (XRD) was conducted on all samples collected from all the different lava tubes outlined in Table 1. Analyses show that, throughout the different lava tubes situated in the park, the speleothems had similar composition. Amorphous silica was present in all the samples collected, with a typical dominant broad peak observed at 21.74° to 22.00° 2θ CuK α (Jones et al., 1964). Chalcedony was detected in some of the samples through XRD with sharper peaks at the same 2-theta as the amorphous silica, and later verified optically through a petrographic microscope due to its fibrous crystal aggregates, sweeping extinction, very low birefringence, and uniaxial/+ optical character. Sharper peaks in XRD at the same 2-theta indicates more order in the mineral, which indicates both the amorphous nature of the opal and the more structured nature of chalcedony. Calcite was also detected in some of the samples in several of the caves but was less prevalent than the silica species (Figure 2). Six out of the nine samples that contained enough calcite for analysis were samples from coralloids growing on the ground of the caves. Almost half the samples collected across all the caves contained only opal, a third of the samples contained opal and a more ordered form of silica (chalcedony), and less than a quarter of the samples contained both opal and carbonate in significant enough proportions to be detected. By weight percent, the samples with opal and carbonate only contained on average 11% ± 4% carbonate.

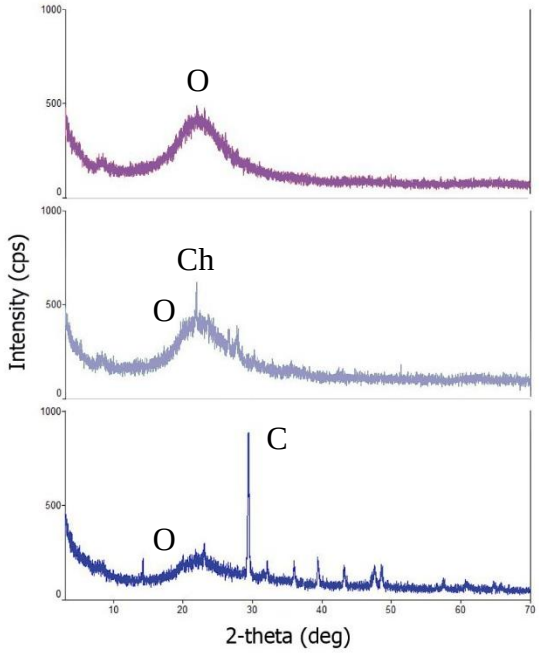

Figure 2 Common XRD patterns from all speleothems sampled. O - opal, Ch - chalcedony, C - calcite.

Under a scanning electron microscope (SEM), the amorphous nature of the opal was confirmed as the botryoidal, spherical texture was observed throughout the samples, with no crystal structure observed in the mass (Figure 3). Spheres of varying sizes (0.2 to 7 μm) were observed within samples as well as across different samples. The size and ordering of these amorphous silica spheres are dependent on many factors and will be further explained in Section 2.6.1.1 and 3.4.1. In hand specimen, the samples look opaque to translucent and range from white to dark brown in colour. Silica spheres in the collected samples observed under SEM are well ordered, irregularly arranged, and uniformly sized round particles. Silica spheres also appear to aggregate, and the arrangement is not tightly packed, nor suggest planes of growth on the microscale.

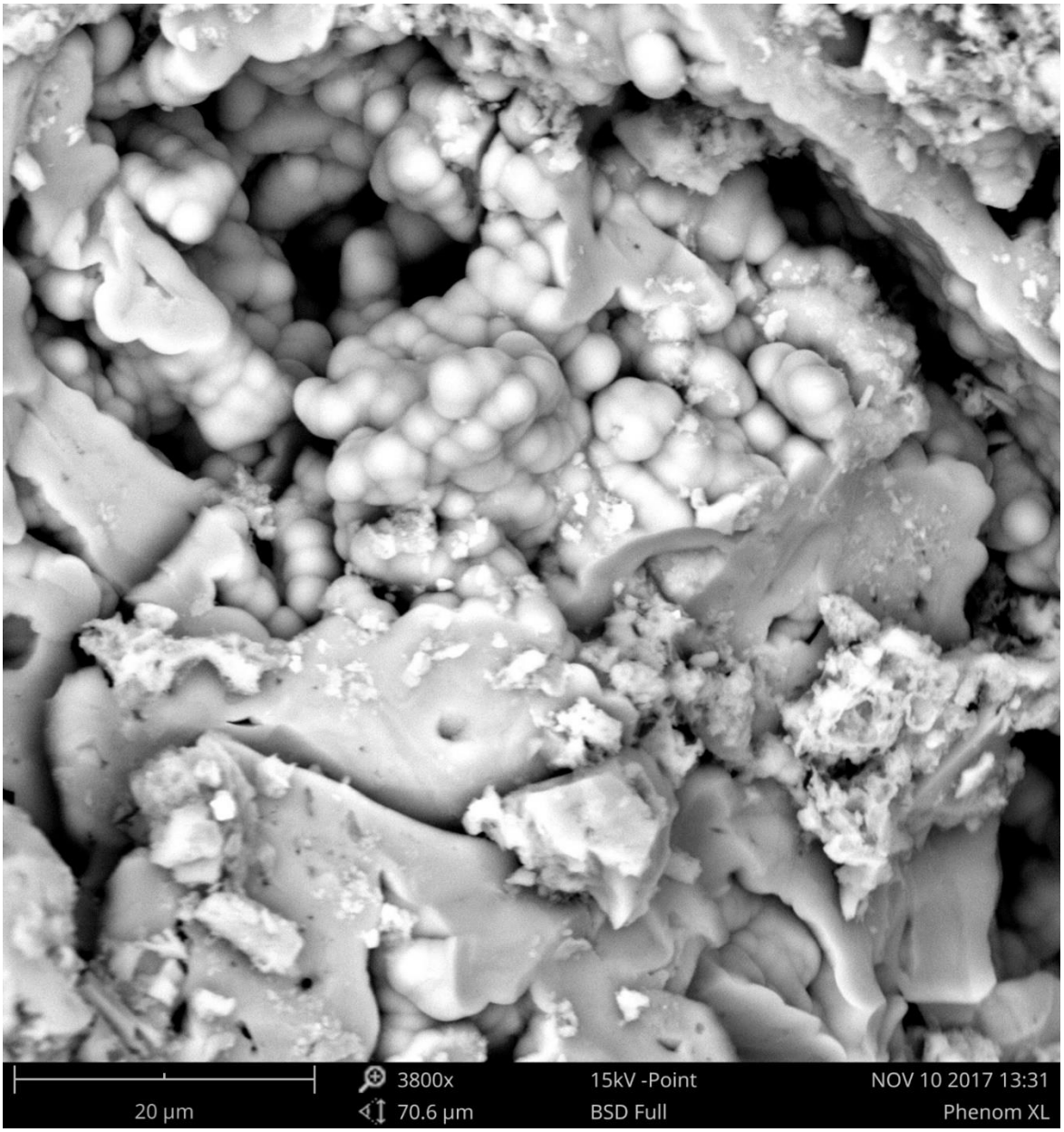

Figure 3 SEM image of the inside of a coralloid speleothem sample showing spherical amorphous silica

2.5.3 Geochemical Analysis

The geochemistry of the cave waters in present day was analysed to understand the formation processes and what is present in the system (Figure 4). From the plot that Si is the ion in highest abundance followed by Na, Ca, Mg in the present-day waters. The alkalinity of the

drip water samples had an average alkalinity of 497.6 ± 244.2 µmol/kg and the pool water samples had an average alkalinity of 822.6 ± 206.3 µmol/kg. The mineral deposits are silica-rich and dominant in the amorphous forms and from the cave waters sampled, the geochemistry of the water seems to be consistent with the speleothem mineralogy, with dissolved silica abundant in the water as well.

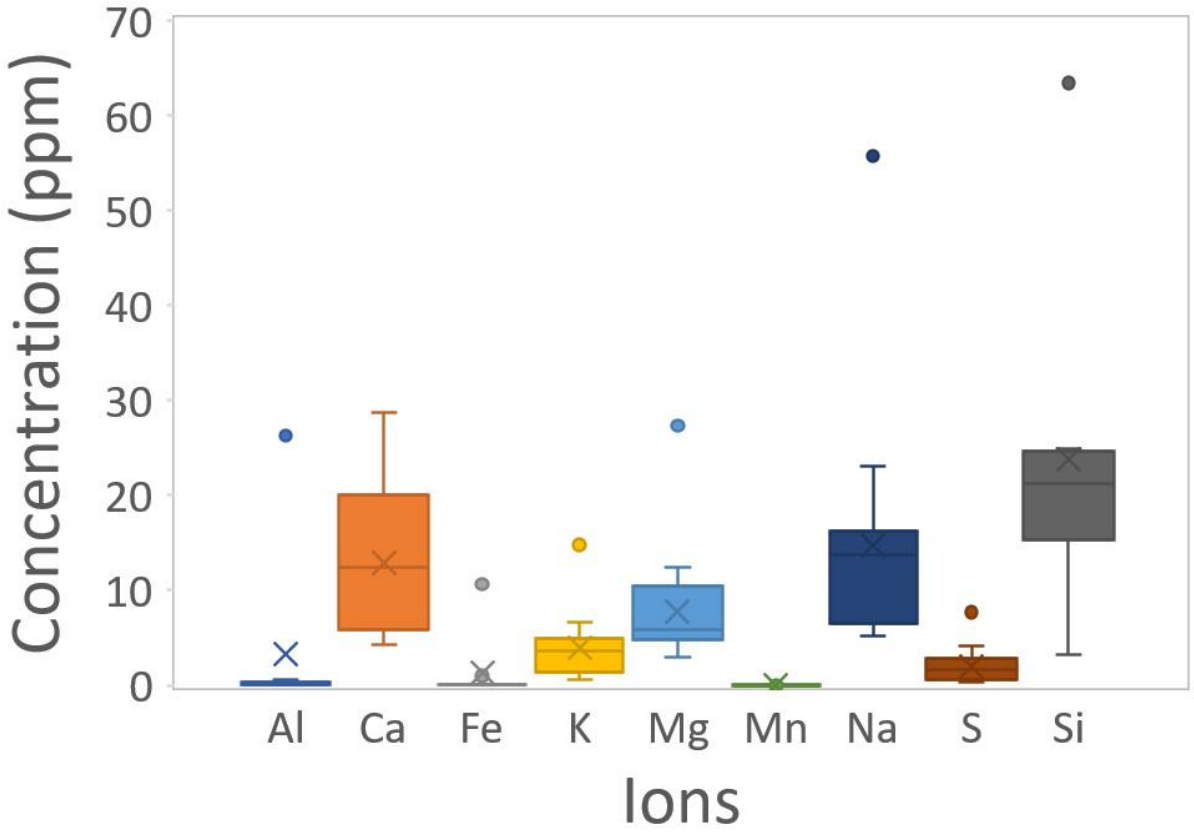

Figure 4 Concentration of ions in cave waters from LBNM. Number of samples for all ions were the same, mean concentration is represented by the X, the middle line of the box is the median, top line of the box is the third quartile, bottom line of the box is the first quartile, whiskers indicate variability outside the first and third quartile and outliers are represented by the points.

2.5.4 Isotopic Analysis

Water was collected and $\delta^{18}O$ and δD were plotted to identify the source of water that is present in the caves (Figure 5). The samples from the first two field seasons generally follow the global meteoric water line (GMWL), but the majority lie slightly to the right of it. This indicates that both the drip and pool water sampled inside the cave reflect the isotopic composition of the meteoric water of the region. The trend of points to the right of the GMWL is indicative of an evaporative setting, which is a common process in caves. Furthermore, it appears that both the drip water and pool water samples cluster in groups. It is seen that the water samples collected from the ice caves are more enriched in both $\delta^{18}O$ and δD in comparison to water samples collected from caves that contain large numbers of coralloid speleothems. In the field, in caves with perennial ice, there are fewer coralloid speleothems found.

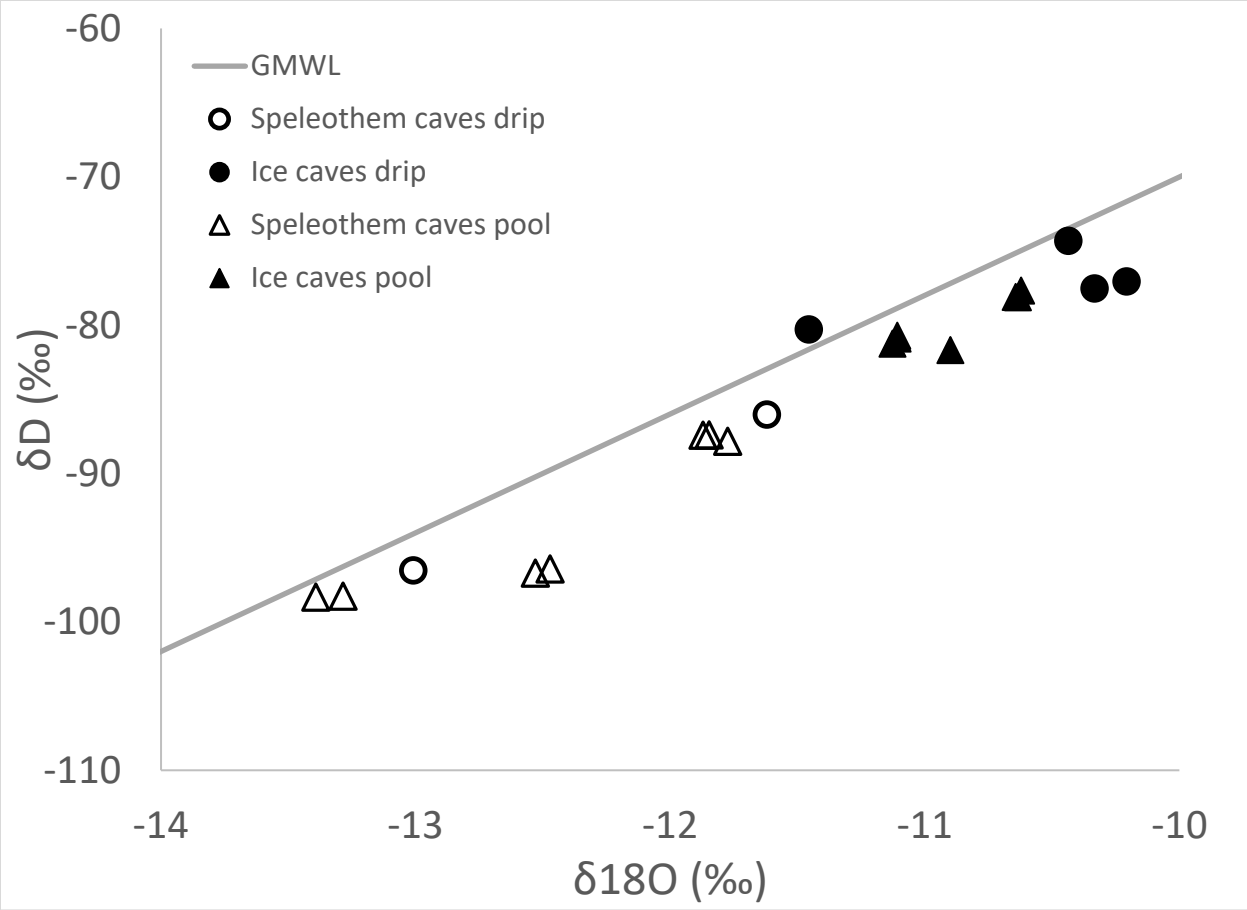

Figure 5 Graph of δD vs δ18O for pool and drip water samples collected from various caves. Filled in points are waters obtained from caves with perennial ice, empty points are from caves where there is a lot of speleothem growth. Triangles indicate drip water, circles indicate pool water.

The different isotopes analysed in the rest of the system are summarised in Table 2. Not all speleothem samples had enough carbonate to for carbonate isotopic analysis. Other materials within or above the caves have also been analysed for $\delta^{13}C_{org}$ and $\delta^{15}N_{org}$. Total C, organic C and N are also quantified to describe the system. In isotopic analysis of aliquots of the same samples, the inorganic and organic fractions of the coralloid speleothems show an approximately -27.6‰ difference (Figure 8). The average value for $\delta^{13}C_{org}$ is -24.7‰ ± 1.1, and the average value for $\delta^{13}C_{carb}$ is +2.9‰ ± 0.9. Overlying plant matter had a $\delta^{13}C_{org}$ of -27.9‰ and the overlying top soil had a $\delta^{13}C_{org}$ of -24.9‰. The $\delta^{15}N_{org}$ of the speleothem samples ranges from -0.97‰ to +9.63‰.

*Table 2 Summary of isotopes of carbonate and organic matter, TC, TOC, TN of speleothems, along with other materials collected in relation to the system. Uncertainties for isotopic analysis are as follows: ± 0.05‰ for $\delta^{13}C_{carb}$ and $\delta^{18}O_{carb}$ v VPDB; ± 0.1‰ for $\delta^{13}C_{org}$; ± 0.6‰ for $\delta^{15}N_{org.}$ *TOC numbers with asterisk are over the TC, these numbers are higher due to margin of error related to analysis, the interpretation for these samples is that there is high amount of TOC in the sample.*

	Description	**δ18O carb**	**δ13C carb**	**δ13C org**	**δ15N org**	**TC**	**TOC**	**TN**	**C/N**
CRF_C2	Ceiling	-9.77	2.47	-27.1	-0.59	1.28	0.6	0.08	7.2
CRF_C3	Floor	-10.38	2.09	-23.8	4.36	0.95	0.8	0.10	8.2
CRF_C4	Floor	-	-	-25.2	6.26	1.28	1.0	0.12	8.4
CRF_C5	Floor	-	2.7	-23.5	6.44	4.51	2.1	0.14	14.6
CRF_C6	Unknown location	-9.92	4.28	-	-	-	-	-	-
CRF_C21	Ceiling	-	4.0	-24.6	5.63	2.28	0.9	0.10	8.3
CRF_C22	Ceiling	-	2.0	-26.6	2.20	5.36	1.7	0.15	11.1
YEL_C0	Floor	-9.17	3.64	-	-	-	-	-	-
YEL_C1	Floor	-8.83	2.54	-23.7	6.58	1.46	1.1	0.10	10.4
YEL_C2	Floor	-	-	-24.3	7.65	1.10	1.0	0.10	10.5
YEL_C3A	Ceiling	-	-	-24.5	-0.97	1.44	1.4	0.18	7.5
YEL_C3B	Ceiling	-	-	-23.7	1.87	1.34	1.1	0.14	8.3
YEL_C5	Ceiling	-	-	-25.6	0.64	1.07	1.0	0.16	6.4
YEL_C6	Floor	-10.24	2.15	-23.7	9.63	9.37	7.2	0.80	8.9
YEL_C8	Ceiling	-	-	-25.3	-0.07	1.03	0.9	0.13	6.8
YEL_C22	Ceiling	-	-	-24.4	2.92	0.54	0.6*	0.08	7.8
CRF_T1	Overlying soil			-24.9	2.07	4.34	4.3	0.17	25.3
YEL_S22	Cave mud			-35.0	-1.26	1.07	0.6	0.11	5.8
YEL_S23	Cave mud			-31.8	4.38	0.17	0.3*	0.04	7.0
P3	Overlying plant			-27.9	-1.47	44.02	44.0	1.70	25.9

2.5.5 Surface microbial features

There are several microbial cellular morphologies observed on the surface of the speleothems using a SEM (Figure 6). Areas where biofilms can be identified without a microscope were targeted; however, through SEM microbial morphologies can be detected throughout the surface of the samples. Filamentous bacteria are most commonly seen, occurring often with other forms of bacteria as well on its own. Microbial forms are mostly seen in

clusters. On the surface, microbial morphologies are seen with the amorphous silica texture but retaining the form of the microbial morphological structures prior to being silicified (Figure 7).

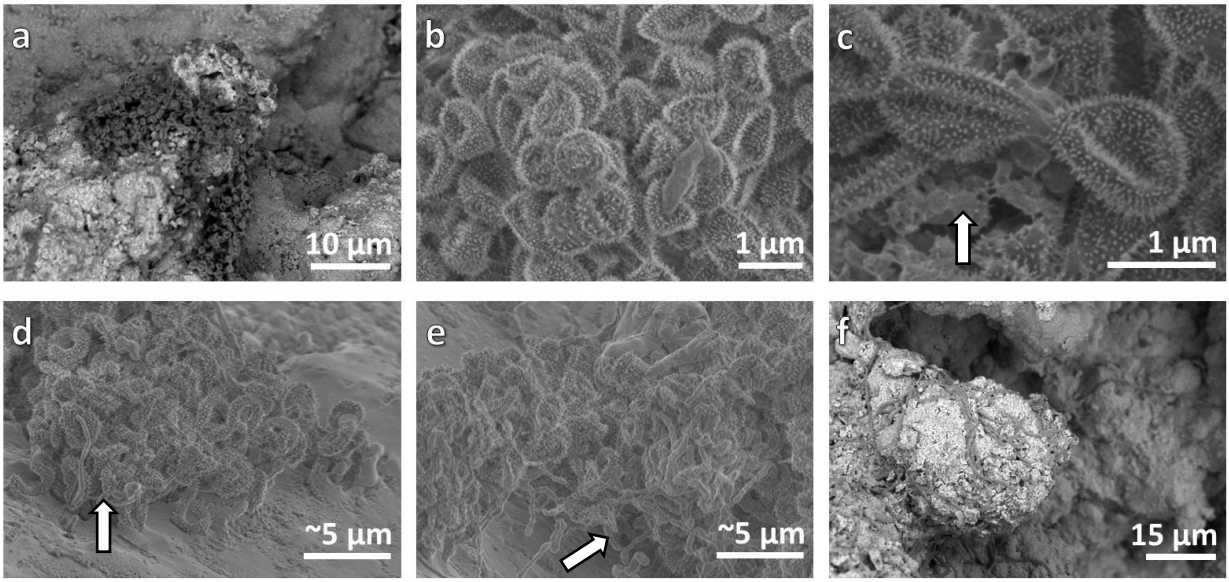

Figure 6 Microbial morphological types seen on the surface of speleothems collected from YEL and CRF lava tubes. 5a shows clustering of coccus shaped bacteria in the center of the image. 5b and 5c shows a zoomed in view of 5a, further showing the clustering nature of the coccus bacteria, with 5c showing amorphous silica in the lower left corner (arrow) showing the close relationship of the two even at micro scales. 5d and 5e different areas of the same cluster of spirochete forms, filamentous forms are seen throughout and exemplified best in 5e (arrow) and bacillus form seen in bottom left corner of 5d (arrow). Finally, in 5f, we see clusters of filamentous bacteria on their own.

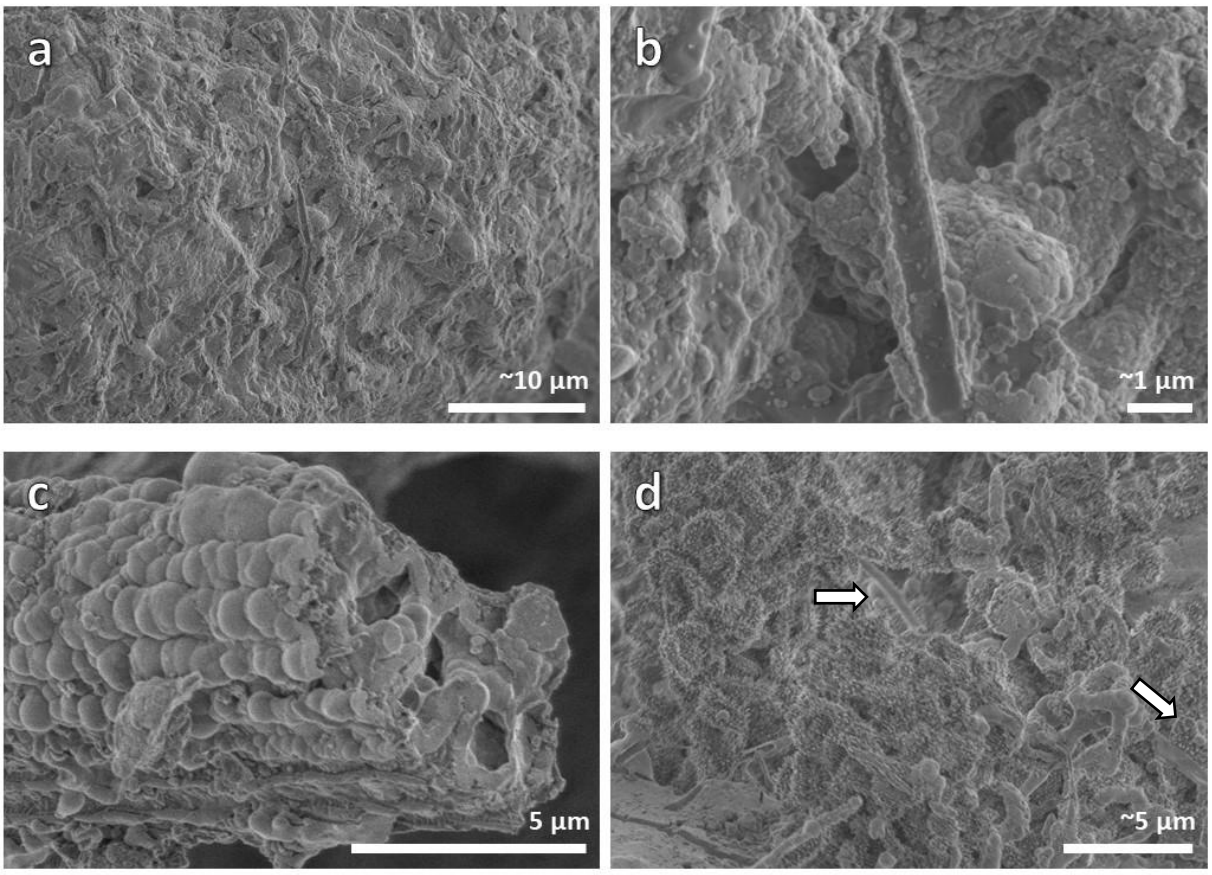

Figure 7 Microbial morphological features showing silicification. Amorphous silica seen throughout the sample is seen having taken on microbial structures. Figure 7a shows a previous filamentous mat that is silicified, and 7b is a zoomed image of 7a showing the details of the botryoidal texture. Figure 7c shows a tubular structure that also appears to have been replaced by silica spheres. Figure 7d shows small spheres of silica at the base of and in small sections of an unsilicified surface microbial feature (arrows), possibly showing the process in which these surface features become overtaken by amorphous silica.

2.6 Discussion:

2.6.1 Physical biosignatures

Silica fossilization is a process that occurs in many environments of the world since silica is a common component of Earth's chemistry. This is a well-known process for preserving fossils on Earth ranging from the Cambrian to the Paleogene (Schubert et al., 1997). It is also

seen occurring in many different environments on Earth, from marine settings in the presence of chert nodules of preserved sponges, to continental settings with the presence of petrified wood (Senkayi et al., 1985; Kidder and Erwin, 2001). Silica fossilization is also important in preserving trace fossils in the form of burrows and bioturbations (Buatois et al., 2017). The use of silica deposits for detecting possible fossil life on Mars has already been discussed due to hydrothermal features found on Mars (Preston et al., 2008).

Fossilization of microorganisms have been reported prior in carbonate speleothems in karst caves (Jones and Motyka, 1987; Jones, 2001). Coralloid samples from an Easter Island lava tube examined under FESEM showed mineralized tubular sheaths and opal-A microspheres clustered on microbial mats and filaments (Miller et al., 2014). Amorphous opal spheres appearing with microbial clusters are also confirmed in this study (Figure 7d). Since speleothems reflect the host rock chemistry, lava tubes on Earth contain more silica rich secondary mineral deposits in comparison to more abundant carbonates or sulphates in limestone or dolomite caves (Hill and Forti, 1997; Woo, 2005). This is a good analogue for Martian lava tubes, which are also hosted in basaltic lava fields, and it is expected that through hydrologic processes the water-rock interaction would form speleothems that are more silica rich. In silica-rich terrains, 20-30 mg/L of dissolved silica in neutral pH groundwaters is commonly seen (Aston, 1983). Our caves report dissolved silica content in the cave waters at an average of 24 ppm; in other caves with silica-rich speleothems, dissolved silica content has been reported to be as low as 3-12 ppm (Wray, 1999).

2.6.1.1 Opal chemistry

The opal structure may also provide contextual information about the hydrologic and geochemical processes. The layered crystal growth of the concentric structure of the opal

indicates that it forms in environments with low growth rates compared to radial growth which is typical of higher growth rates (Sunagawa, 2005; Gaillou et al., 2008). In addition, when there is a high concentration of silica, irregularly stacked spheres occur possibly due to nanograins having limited mobility causing aggregation (Gaillou et al., 2008). The opal structure and phase might also indicate something about the pH and ionic strength at the time of the formation, silica colloids assemble between pH values of 1 to 3.5 and then again from 9.5 to 10.5 (Piret and Su, 2008). In addition, the opal phases can indicate information about the formation history since amorphous opal gradually transforms to higher order microcrystalline quartz through diagenesis (Liesegang et al., 2018). Since this transformation depends on dissolved silica source, particle density, and most importantly, water content, information regarding the hydrogeologic history can be inferred (Herdianita et al., 2000; Liesegang et al., 2018). Opal phases are further discussed in Section 3.4.1.

2.6.2 Isotope Geochemistry of Speleothems and Related Materials

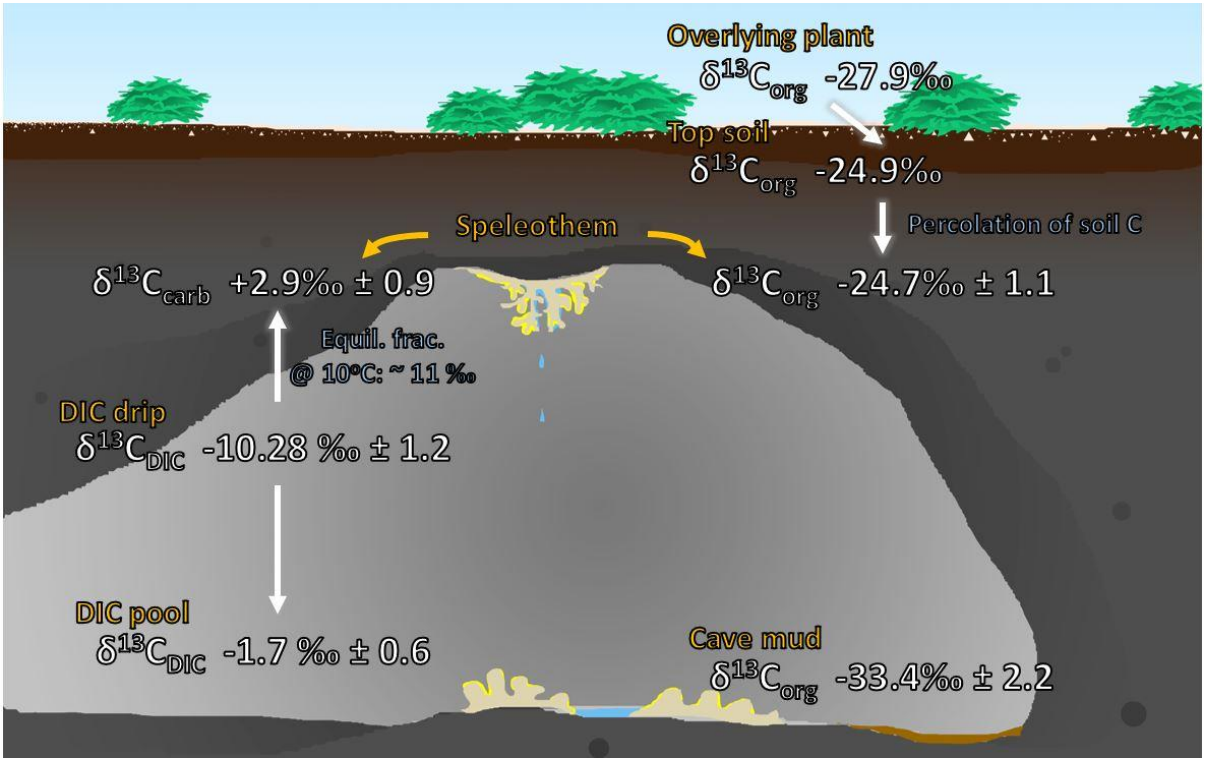

Figure 8 Schematic diagram of isotopes analysed from samples collected in the lava tubes at LBNM. Lava tubes are basaltic rock and are usually 1-2m thick overlying the cave ceilings. Average isotope values are displayed with standard deviations of multiple samples.

The range of $\delta^{15}N_{org}$ values is ~ 10.6‰, which is considered a large range for adjacent samples collected under similar abiotic influences. The $\delta^{15}N_{org}$ values suggest that there has been recycling of organic material occurring due to the large range of values in comparison to the range of values for the $\delta^{13}C_{org}$. This is a typical isotopic pattern observed in soils, with strong enrichment of $\delta^{15}N$ and more moderate enrichment of $\delta^{13}C$ with soil depth (Natelhoffer and Fry, 1988). The huge range of $\delta^{15}N$ values also could suggest different trophic levels or different metabolic pathways being recorded in the OM in the speleothems. We hypothesize that the source of organic carbon in the speleothems is derived from overlying plant-derived carbon that has been recycled by heterotrophs in the overlying soil and has percolated into the cave,

presumably as dissolved organic carbon. Figure 9 shows further evidence that there is a link between the organic source of the overlying plant and soils and the speleothems within the cave, in that the speleothem organic matter falls on the same slope as the plant and soil organic matter in a plot of $\delta^{13}C$ and $\delta^{15}N$. This implies that the speleothem organic carbon is predominantly derived from the soils. From the C/N vs $\delta^{13}C_{org}$ plot (Figure 10), it is seen that the samples of material overlying the caves have higher C/N ratios in comparison to all the samples from within the caves. This suggests that not all the organic matter from the surface is being transferred or reflected in the organic matter that we see in the subsurface. In both Figure 9 and Figure 10, cave mud is much more depleted in ^{13}C compared to other samples, suggesting a distinct primary carbon source and/or different microbial communities producing the organic matter in the mud. Two possible sources of this ^{13}C depleted organic matter are methanotrophic or lithotrophic microbes (Webster et al., 2016; Lennon et al., 2017), although more work is required to evaluate this hypothesis.

The C/N values of the organic component in the speleothems, 6.4 - 14.6, is in the range expected for bacteria and algae (generally 4-15), since these measurements were done on aliquots, the isotope values are assumed to reflect microbial organic matter. The cave mud samples had C/N ratios of 5.8 and 7.0 which are slightly lower than the average C/N for the speleothems which is 8.9 ± 2.1. The overlying top soil and plant had C/N ratios of 25.3 and 25.9, respective. The C/N in the speleothems is lower than the overlying soil, implying that there is further recycling as OM moves down into the cave. The influence of plant matter is not reflected in the C/N ratios of the speleothems, meaning plant matter is not transferred down into the caves despite similar isotopic values. Comparing our C/N ratios to other basaltic caves in Hawaii, Léveillé et al. (2007) reported average ratios of 13.5 ± 5.1, which is higher than our average of

8.9 ± 2.1. Their cave system was not completely in the twilight zone, and photosynthesis was occurring. This might contribute to the higher C/N ratios as photosynthesis is directly related to increase in C/N due to increase in cell-wall polysaccharides (Torres et al., 1991). In addition, Miller et al. (2016) reported average C/N ratios of 5.3 ± 0.5 from lava tubes on Easter Island, which are lower than our values. In further comparison of %C and %N between this study and the other two sites, averages of: 1.05%C and 0.13%N; 9.1%C and 0.8%N; 4.8%C and 0.9%N were reported for this study, Léveillé et al. (2007), and (Miller et al., 2016), respective. Our site, even in comparison to other basaltic caves, has low %C and %N. This could possibly be due to climatic effects as the other two sites are in more tropical climates, thus leading to higher productivity in those environments in comparison to LBNM which is a semi-arid desert at moderate altitude. The more tropical climates also are expected to have larger soil horizons, which affects the amount of carbon above the caves that can be transported in through percolation. This smaller reservoir of carbon could also be the reason why there is favoured precipitation of silica-rich deposits, instead of carbonates, within the caves, because of DIC being a limiting source.

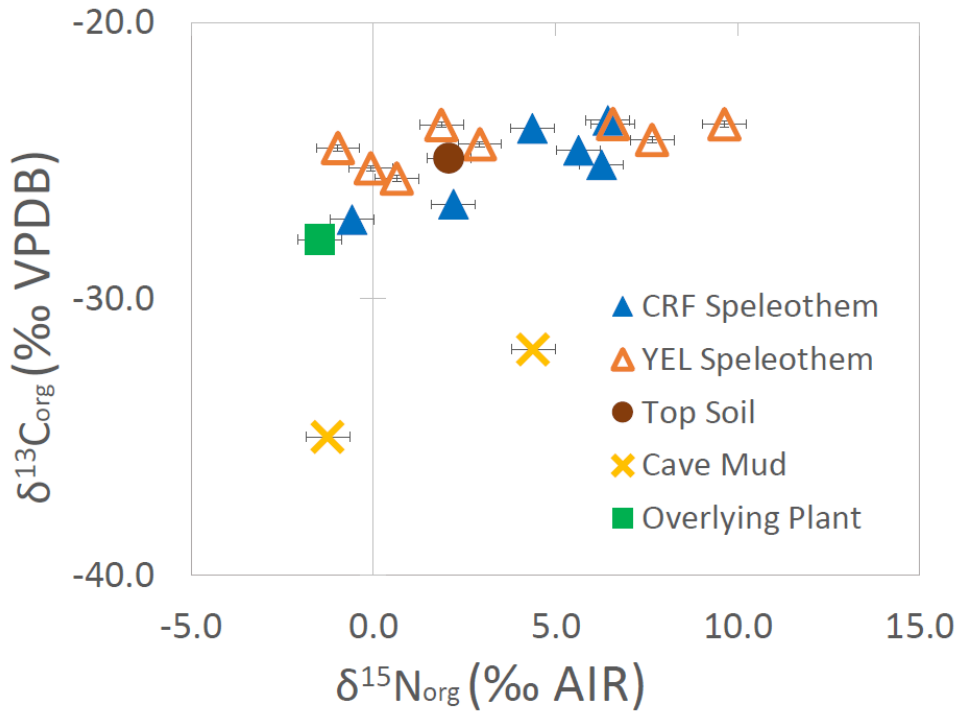

Figure 9 C vs. N plot showing a positive trend in two systems: the first correlates the overlying plant and soil with the speleothems, and the second shows a separate signature for the cave mud.

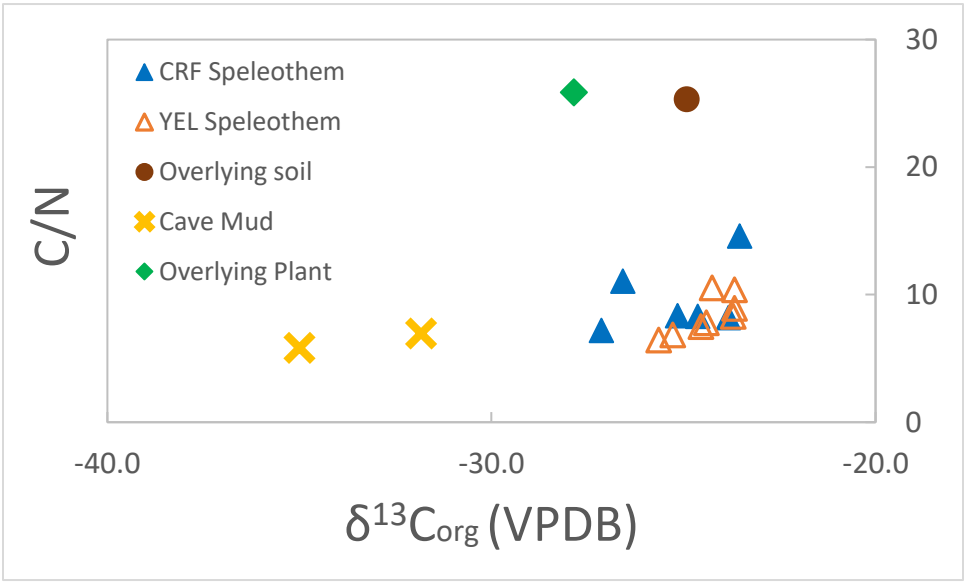

Figure 10 C/N vs 13C$_{org}$ plot showing the higher C/N from the overlying materials sampled, and plant matter C/N reflected in overlying soil. The plant matter with higher C/N ratios has not been transferred down through the cave, as all materials from the cave are lower in C/N.

The $\delta^{13}C_{carb}$ fraction in the speleothems is also enriched compared to the expected value for equilibrium in the cave. There is about a +13.18‰ enrichment from the DIC in the drip waters to the speleothems (Figure 8). The caves have a moderate and regular temperature year-round, so based on the temperature measurements taken at the caves when sampling was done, a value of 8°C has been assumed for equilibrium calculations. Based on this assumption, the speleothems are between 1-2‰ enriched in comparison to formation at equilibrium based on Kim and O'Neil (1997) (Figure 11). This enrichment could be due to kinetic degassing or possibly local microbial induced fractionation. To definitively conclude a microbial signature, the base DIC isotopic signature needs to be established year round in order to determine if the enrichment is due to a seasonal or other abiotic effect (Sumner, 2001). The stable isotope analysis for the DIC in pool water was conducted in early spring whereas the DIC in drip water was collected and analysed mid-summer. The change in seasonal drip water in a limestone cave in China between spring and summer was about -1 to -2‰, whereas the difference for the pool water was -1‰ (Wu et al., 2015). Our $1000Ln^{18}O_{carb}$ in our caves was on average 33.7‰ ± 0.5, and under equilibrium conditions, a value of ~31.7‰ is expected in our caves based on Kim and O'Neil (1997). This observed enrichment of ~2‰ could also be due to kinetic effects related to degassing of DIC which is consistent with the positive correlation between $\delta^{18}O$ and $\delta^{13}C$.

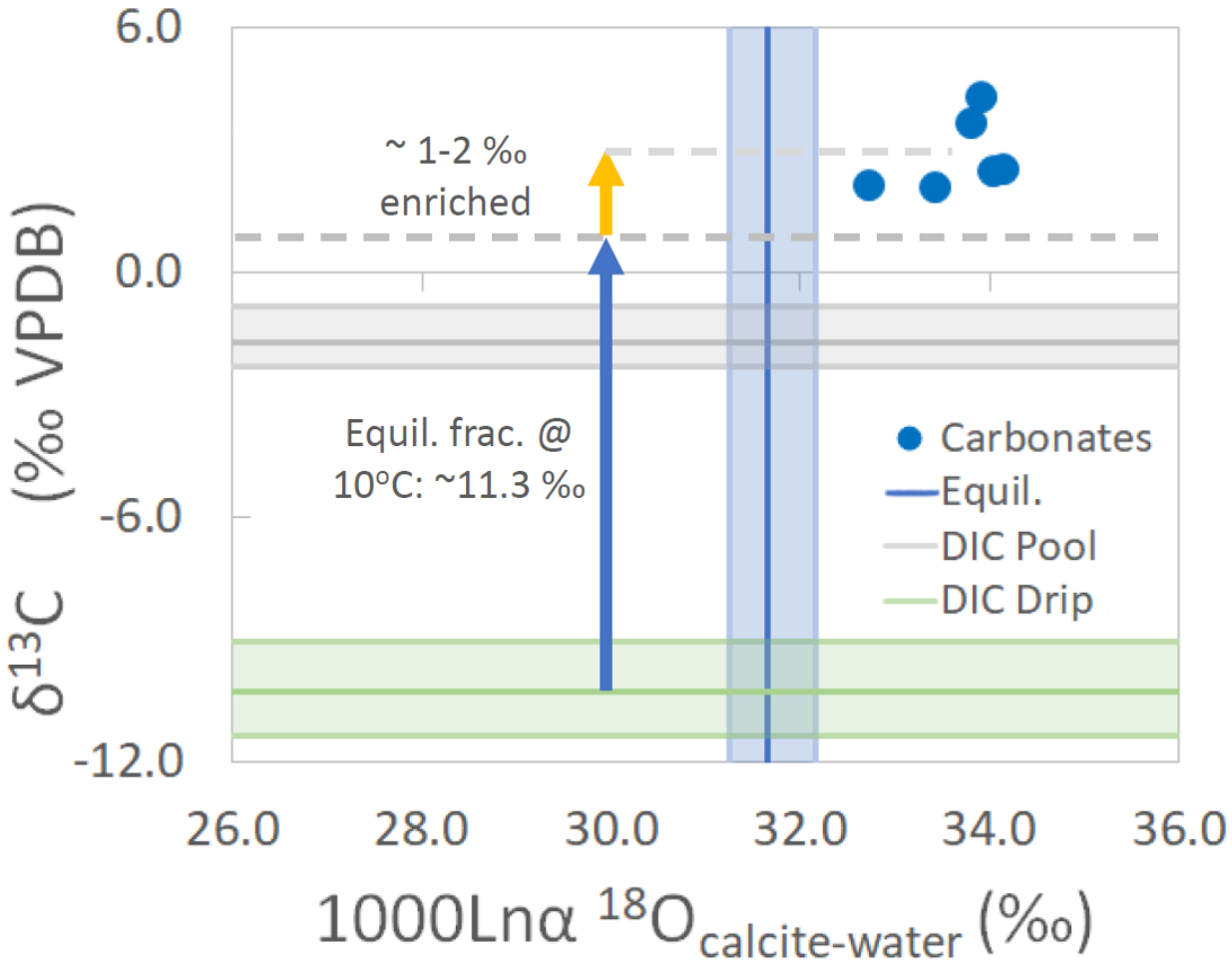

Figure 11 ^{13}C vs ^{18}O plot of carbonate fraction of speleothems with comparison to DIC in cave waters. Equilibrium calculation based on temperature of 8 °C ± 2°C.

2.6.3 Comparison of speleothems based on location within and between caves

The isotopic values of the organic carbon in the speleothems are statistically different between the floor and ceiling samples ($p<0.05$) (Section 2.9: Table 3). This suggests that there are different organic sources for the speleothems from the cave ceiling and the floor. In contrast, the isotopic values of the inorganic carbon fraction of the speleothems sampled from the cave ceiling and ground are statistically indistinguishable ($p>0.05$), despite different isotopic

signatures of the reservoirs (cave drip versus pool). This could be due to a seasonal difference in sampling the pool and drip waters for DIC or it could possibly reflect different processes occurring in speleothem formation (Caddeo et al., 2015; Wu et al., 2015). Also, interestingly, between the two different caves (YEL and CRF), the inorganic C portion of the speleothems are indistinguishable ($p>0.05$). This suggests that even though the caves are situated in different lava flows, and in different cave systems, there are similar sources and/or formation processes resulting in the same isotopic signature. In a dolomitized carbonate cave in Italy, subaerial and subaqueous formation of carbonate speleothems lead to different stable isotopes signatures (Caddeo et al., 2015). The subaqueous coralloids were collected from pools, and the subaerial coralloids were collected from the cave ceilings or walls and that will be the basis for the comparison between their study to this study. Caddeo et al. (2015) found in their cave that in subaqueous coralloids, $\delta^{13}C$ and $\delta^{18}O$ were 12-15‰ and 4-5‰ less, respectively, than that of subaerial coralloids. In our caves, the coralloids from the ceiling are formed subaerially; however, it is uncertain from observations in the field if the pools of water within the caves would sustain continuous subaqueous growth of the coralloids from the ground, but the more positive $\delta^{13}C$ values seem to agree with both our ceiling coralloid data and Caddeo et al.'s (2015) that the speleothems from the ground mainly grew under subaerial conditions. If we assume that both our ceiling and floor samples are formed subaerially, they would be expected to have different $\delta^{13}C$ values as the reservoirs of water in which they are formed have different isotopic signatures (pool water average: 1.70‰; drip water average: -10.3‰). Our speleothem samples are indistinguishable by the $\delta^{13}C$ values in the carbonate fraction. If the samples were formed at equilibrium for both conditions, to produce similar $\delta^{13}C$ values of carbonates, the carbonates formed in pool water would have undergone a process that fractionated the samples by -7.8‰

and the carbonates formed in drip water would have fractionated by +1.62‰ (Figure 12). Further work in stable isotope analysis along and across the direction of speleothem formation would help to determine if formation mechanism was a major factor in ^{13}C in carbonate signature in predominantly silica-rich deposits.

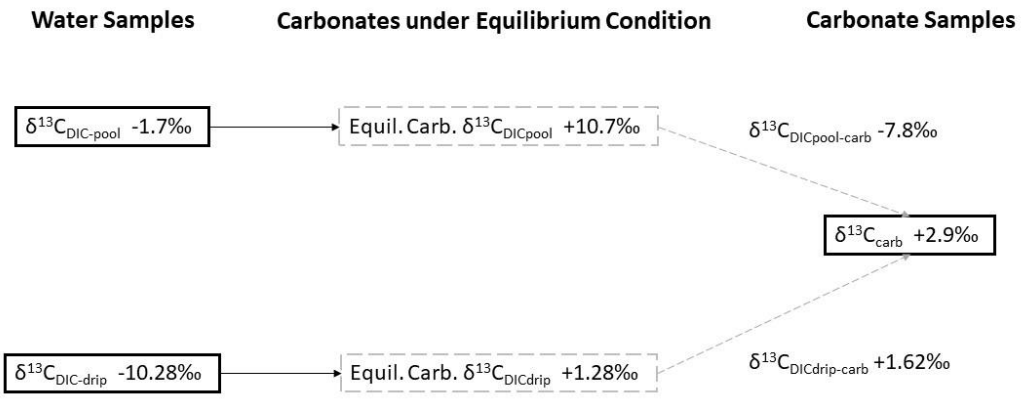

Figure 12 Diagram showing relation of DIC water reservoirs, carbonate samples and calculated equilibrium precipitation of carbonate from DIC in water reservoirs from LBNM. Black boxes indicate measured values from samples collected, grey dashed boxes are expected values of 13C in carbonate formed at equilibrium based on measured DIC samples.

2.6.4 Approach for Mars sampling

If liquid water existed in the subsurface of Mars (Ehlmann et al., 2011), it is possible that similar precipitation and evaporation processes have allowed for the growth of cave mineral deposits. Coralloids are common speleothems on Earth that commonly grow due to thin films of water, in comparison to larger speleothems like stalagmites or stalactites which grow in larger volumes of water (Hill and Forti, 1997). It is seen through this study and other studies on Earth of coralloids in basaltic lava tubes, that the composition of the secondary mineral deposits is varied depending on the composition of the host rock, the air conditions inside the cave, the

amount of water available, and the materials lying above the cave that leech into the caves through water transport (Hill and Forti, 1997; Woo et al., 2008; Miller et al., 2016; Vanghi et al., 2017). Based on conditions we know about speleothem formation and basaltic lava tubes on Earth, we can examine if Mars had similar conditions in the past.

2.6.4.1 Implications of speleothems from Lava Beds National Monument

From this study, based on $\delta^{18}O$ and $\delta^{2}H$ isotopes of cave water plotting on the GMWL, we know the source of water in the caves is from meteoric water that has seeped in through host rock. The cave water geochemistry also indicates weathering of the host rock as it contains elements expected from the weathering of a basalt, with the highest concentration being dissolved silica. The field readings of pH in cave water from LBNM ranges from slightly acidic to slightly basic, which is within the range of hydrological conditions for deposition of silicate cave minerals (Hill and Forti, 1997). In this study, we also see that the composition of the coralloids hosted in a basaltic lava tube, is very silica rich, with only minor calcite. This might make lava tubes at LBNM a more comparable site for analogue studies for Mars as it is a semi-arid desert environment with almost no soil horizon on site. It is a less productive region than other studies of lava tubes in tropical environments, which might be more similar to Mars.

2.6.4.2 Conditions needed for biosignature preservation in speleothems in lava tubes on Mars

For detection of biosignatures on Mars, the first thing that is needed is for life to have existed, but also in a form that is similar enough to life on Earth in order to increase the chances of our developed methods to detect it (Abrevaya et al., 2016). Next, we see from this study that in present day, the speleothems are covered in biofilms, and we see evidence of the biological structures of these biofilms being preserved on the surface of the speleothem through

silicification (Figure 7). This indicates that for any possible biosignatures to be preserved, there has to be concurrent growth of the speleothems with the presence of biology within the same period of time. This is also seen with the $\delta^{15}N$ and $\delta^{13}C$ isotopes which indicate that the primary source of organic matter found in the speleothems is soil organic matter transported from the surface, with the soil organic matter having been reworked from plant organic matter. Lastly, we see a correlation of fluorescence signatures that indicate organic matter, relation to certain mineral layers in the speleothem (refer to Chapter 3). Another condition for biosignature preservation to be detected on Mars, is liquid water, as it is also a condition for speleothems to form. Lastly, for any missions to successfully detect biosignatures on Mars, there needed to have been no destructive processes that occurred between the time of biosignature preservation until sampling takes place.

2.6.4.3 Possibility of Mars having conditions for speleothem formation and biosignature preservation in lava tubes

Lava tubes have been found in many volcanic regions on Mars, which is expected as they are common features in volcanic regions on Earth (Cattermole, 1990; Bandfield et al., 2000; Bleacher et al., 2007; Leone, 2014). From the few samples of Mars basalt from meteorites that have been analysed, it is seen that the basalt from Mars is comparable to Earth end-member oceanic island basalts and mid-ocean ridge basalts (Greenough and Ya'acoby, 2013). It is unlikely that this is representative of basalt composition on Mars as a whole, but it is important that analogue studies on Earth are in environments which will match the composition of the host volcanic rock on Mars. In this study we see that amorphous silica is the major component in speleothems in lava tubes at LBNM, and silicate cave minerals in general are commonly formed

in volcanic host rock caves (Hill and Forti, 1997), so it can be assumed that silicates will be a major target for lava tube exploration.

One of the most important processes that must be present for speleothem formation is liquid water. This is seen in all modes of speleothem formation on Earth, whether it be through capillary water, ground water seepage, aerosol transport or another mechanism (Hill and Forti, 1997). Advances in research and modelling for Mars in recent years have pointed to a warmer, wetter Mars in its early history (Carter et al., 2015). Proposed models of the Noachian to early Hesperian, indicate the presence of ground water as well as episodic presence of liquid water on surface (Ehlmann et al., 2011). Although it's not exactly known what might have caused the presence of water then, there are several possible mechanisms that existed around the time that could have contributed to the melting of ice: widespread volcanism, planetary geothermal gradient and heavy impact bombardments (Abramov and Kring, 2005; Coleman et al., 2007; Parmentier and Zuber, 2007; Schwenzer et al., 2012). During the Noachian, basaltic rocks were thought to be highly permeable on a macroscopic scale due to impact and cooling-induced fractures, which allowed for greater chances of fluid water entering the subsurface (Ehlmann et al., 2011). For silicate cave mineral deposition, the water would also have needed to be slightly acidic to slightly basic in order to weather the host rock (Hill and Forti, 1997). Slightly acidic conditions could have been possible on Mars at the time due to volcanic gases, such as H_2S or SO_2 released during eruptions (Ehlmann et al., 2011). Slightly basic water conditions could have also existed on Mars, as carbonates from the Phoenix landing site have shown that they may have formed in-situ through ephemeral water (Niles et al., 2013). With a small sample size of data that has been ground-truthed on Mars, the acidity of waters for the planet is largely unknown but could be similar to Earth where there is a regional effect on water chemistry.

Specifically, for biosignatures to be preserved in speleothems on Mars, if life was ever present, it also would have needed to be active while speleothem formation is active (Toporski et al., 2002). This is seen in this study, with microbial structures being preserved by amorphous silica in-situ, with both components being present in the system at the same time. If speleothem formation occurred and ended prior to life on Mars, it would not be able to record the presence of life unless said life somehow altered the mineral deposits post-formation. Although, it is likely that if life existed and speleothems formed on Mars, they would have been concurrent, as conditions for both require liquid water and a warmer environment than what is seen present day. However, more research is needed in order to constrain regional and temporal limits for the presence of both speleothems and possible life on Mars. In addition, caves have been regarded as environments where secondary mineral precipitation and microbial growth can be enhanced by stable physico-chemical conditions (Léveillé and Datta, 2010). Having stable conditions might also increase the time of overlap between cave mineral formation and possible microbial life, allowing for more interaction between the two systems.

Lastly, if all previous conditions are met, and cave mineral deposits were able to record the presence of past life, for any future missions to Mars to detect biosignatures, no destructive processes could have occurred between that initial preservation and sampling. As mentioned prior, as lava tubes are subsurface environments, they provide protection from surface erosional processes, harsh surface climatic conditions and radiation – which are all processes that can destroy biosignatures (Léveillé and Datta, 2010). With silicate minerals being more prevalent in volcanic caves, any structures preserved during silicification is also more resistant to weathering or dissolution, especially in comparison to calcification, which allows it to be preserved on longer time scales (Toporski et al., 2002). As well, the geological periods after the Hesperian are

believed to be very tectonically dormant (Léveillé and Datta, 2010; Ehlmann et al., 2011), so the possibilities of later geological processes overprinting any preserved biosignatures is not likely. Most larger impacts on Mars also occurred during the Pre-Noachian and Noachian geological periods, so any destructive processes caused by impacts is also unlikely (Abramov and Kring, 2005; Ehlmann et al., 2011).

2.7 Conclusion

This study examines the mineralogy and geochemistry of speleothems from lava tubes at LBNM and how they play a role in the preservation of biosignatures. The speleothems in basaltic lava tubes have similar bulk geochemical compositions to their host rock, creating silica rich deposits that are effective at preserving surface microbial features. Isotopic evidence from $\delta^{13}C$ and $\delta^{15}N$ isotopes indicate a correlation of surface organic matter influence on the organic matter found in the subsurface speleothems. There is likely a different process influencing the carbon source in the cave mud in this system. Carbonate formation might indicate a local microbial induced signature, but further work in studying the abiotic isotopic signature of DIC is required. Further work in looking at the formation processes of the silica portion of the speleothem is important as most of the speleothem is comprised of the amorphous silica, which will indicate more about the formation history than the carbonate portion. As an analogue study to Mars, it is possible that the conditions for biosignature preservation in speleothems seen at LBNM could have also existed in the past on Mars.

2.8 Acknowledgements

This study was made possible through funding from the Canadian Space Agency's *Flights and Fieldwork for the Advancement of Science and Technology* (FAST) program. Field work at Lava Beds National Monument was generously allowed through the NPS permit: LABE-2016-SCI-0011. Research was made possible through the GEOTOP program.

2.9 Supplementary Material

Table 3 Comparison of isotope values by caves and by location within caves

	CRF vs YEL Speleothem							
	^{18}O		^{13}C		$^{13}C_{org}$		$^{15}N_{org}$	
	CRF	YEL	CRF	YEL	CRF	YEL	CRF	YEL
Observation	3	3	6	3	6	8	6	8
Mean	-10.02	-9.41	2.92	2.77	-25.14	-24.40	4.05	3.53
P-value	0.277		0.818		0.289		0.775	
	Ceiling (C) vs Floor (F) Speleothem							
	^{18}O		^{13}C		$^{13}C_{org}$		$^{15}N_{org}$	
	C	F	C	F	C	F	C	F
Observation	2	4	4	5	8	6	8	6
Mean	-9.84	-9.65	3.19	2.62	-25.24	-24.02	1.45	6.82
P-value	0.659		0.404		0.027		0.0002	

Preface to Chapter 3

Since speleothems are deposits that are formed in layers, they have been often used as a proxy for environmental changes and chronology. This layering can be useful in interpreting the processes that have occurred during the time that the speleothem was forming. In this chapter, we take a closer look at the smaller spatial scale relation of the mineralogy and the organics in these layers, how they might relate to each other, and what information that provides. In addition, this chapter investigates the use of novel methods in detecting biosignatures and organics spatially. It is written as a complementary section for the thesis but will be further developed as a manuscript later. The samples collected for this section are from the same caves as the prior section, and the biggest, and most representative morphologies were saved for the structural analysis of this chapter. Spatial relations were analysed in cross-section by embedding the samples in resin and the methods of laser-induced fluorescence and Fourier-transform infrared spectroscopy were used to map and confirm organic compounds. Raman spectroscopy was also performed to determine the mineralogy. These methods could be used to analyse samples with little preparation in reconstructing biosignatures at a smaller scale.

3: Spatial analysis of mineral and organic components of a speleothem from a basaltic lava tube

Jenny Ni[1], Richard Léveillé[1], and Peter Douglas[1]

[1] Department of Earth and Planetary Sciences, McGill University, Montréal, Québec

Key words: Speleothems, lava tubes, spatial analysis, fluorescence, organics

3.1 Introduction

Speleothems are secondary mineral deposits that are derived by physicochemical reaction from a primary mineral in bedrock or detritus in caves. They are formed in caves from groundwater seepage, water-rock interaction, and precipitative and evaporation processes (Hill and Forti, 1997). Thus, they are reflective of the environment in which they are formed. Speleothems have long been used as paleoenvironmental and geochronologic indicators. As they generally form with the addition of new rings, the spatial relation of rings within speleothems provide important information as climate proxies (Woo et al., 2008; Lachniet, 2009; Blyth et al., 2016). In addition, studying the difference in mineralogy and organics will allow for a complete picture of the association of the biofilms and the mineral formation in these deposits. Laser-induced fluorescence is also a newer method, especially in the applications of detecting spatial trends of organic material. There is benefit to employing this method in astrobiology as it requires little to no sample preparation and is a non destructive method.

3.2 Sample Preparation

Samples were carefully selected from each sample site from the caves. The criteria for the selection process was based on visual inspection of the most structurally and morphologically representative speleothems of each sample site. Samples were then embedded in clear resin pucks and cut along the highest point of the sample perpendicular to the basalt boundary to get a better representation of all the layers in the speleothem.

3.3 Methods and Instruments

Mineral mapping of the cross section of the speleothems was done through: optical microscopy, Raman spectroscopy and the use of known mineral standards. Organic mapping was done using laser-induced fluorescence (LIF).

3.3.1 Laser-Induced Fluorescence

The instrument used in this analysis is a 266 nm Raman system that is custom built on a breadboard optical table operated at York University in the Planetary Instrumentation Laboratory. The instrument and methodology is described in detail by Eshelman et al. (2014). Briefly, this instrument uses a 266 nm Nd:YAG laser, calibrated to a NIST deuterium lamp, in order to excite samples to obtain a fluorescence spectra. This wavelength has demonstrated effectiveness in detection of organic molecules (Eshelman et al., 2014).

Fluorescence signatures obtained were also analysed using time resolved measurements to identify the decay of the signatures detected. This was done with the same instrument; the gate delay was set to 0.5 ns with 80 acquisitions to observe the decay of the intensity over time.

3.3.2 Raman Spectroscopy

Raman spectroscopy was used to determine the spatial distribution of the minerals in the cross section of the samples. Raman spectra were collected using a Renishaw InVia confocal micro-Raman spectrometer with a 532 nm laser and a Leica microscope objective. The spectra were analysed and collected using Wire 4.2 software. The instrument was calibrated using Si standard with peak at 520.5 cm^{-1}. The measurements were made with 10% power and a 2400 l/mm grating system with a 50 µm slit. The mapping was done at 0.5 µm increments. Prior to analysis of measurements, cosmic ray signals were removed from the data manually using the Renishaw WiRE^{TM} software. Mapping was done through comparison of spectra with spectra of known mineral standards obtained from the McGill Redpath Museum. Mineral standards used were quartz, calcite and opal, which were consistently the major components of samples examined through XRD. Opal 1 is a sedimentary opal sampled from a locality in Hungary, it is orange and brown and shows slight banding, XRD analysis confirms it to be opal-CT. Opal 2 is from a sample of an infilled cavity, the sample shows growth of amethyst on the inside, and a ring of white, botryoidal, opaque opal on the outside, XRD analysis reports this sample as opal-A.

3.4 Results and Discussion

3.4.1 Mineral Mapping

Samples from YEL and CRF cave (mentioned in the previous chapter) were analysed with this method due to the banding seen in the cross section of the speleothems (Figure 13).

Bulk mineralogy analysis had been previously performed with powder XRD, and from that analysis it was shown that opal, chalcedony, and calcite were the main minerals in the speleothems. It is seen from the cross section of Figure 13 that there are secondary mineral deposits (brown masses throughout left side) that are also forming within the rough structures of the basalt substrate.

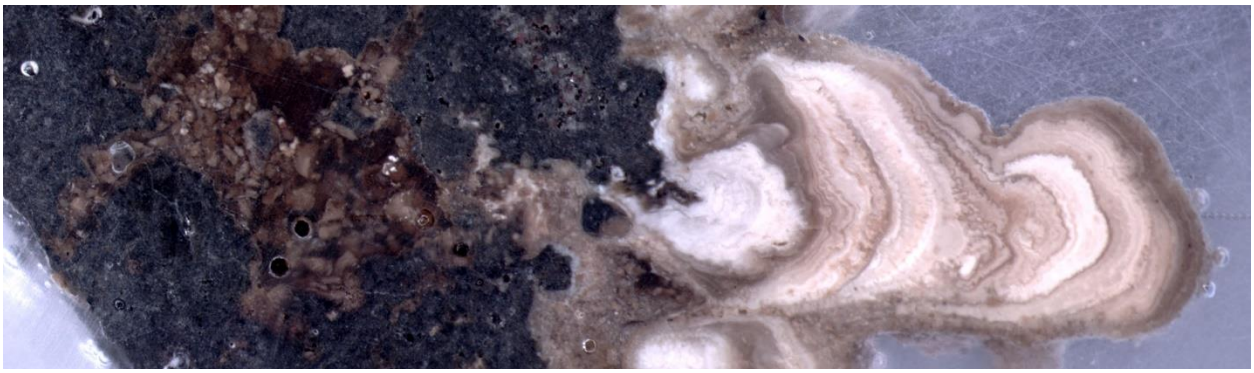

Figure 13 Microscope image of cross section of speleothem. The basalt substrate is seen in black/dark grey, and the brown, beige white sections are the secondary mineral deposit. This sample was a floor sample, the speleothem is growing outwards from the basalt upwards.

The resin pucks were first analysed using a petrographic microscope and layers of growth are observed (Figure 14). From Figure 14, the first image shows lenses of materials that terminate within layers (arrows), possibly former microbial structures that have been silicified in place. The layers are also seen to be very porous, which is expected from amorphous silica that is not well ordered, or possibly from organic structures being cemented. The porous nature of the speleothem is especially prominent in the bands on Figure 14b. In addition, it looks like there are grains of material that have been incorporated within the layers (arrow in Figure 14b).

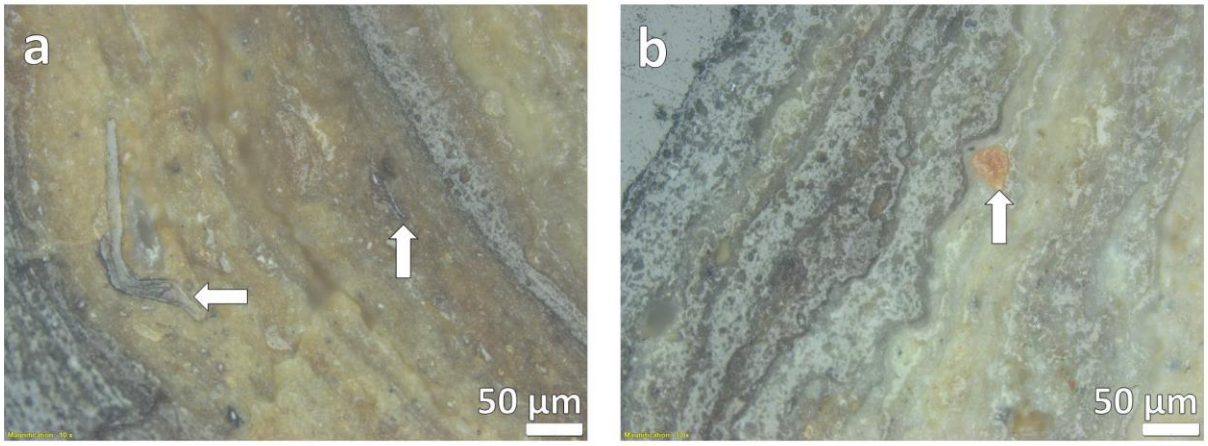

Figure 14 Microscope images of cross section of speleothems that show the textures of the layers within the speleothem deposits

The resin pucks show that there are mineral deposits within the basalt substrate as well as the part that grows out past the basalt boundary as seen in Figure 13. The basalt substrate within LBNM ranges from being very smooth as in the case with lavacicles to being rougher where there are basalt breakdown boulders. The basalt itself appears to be very porous in many of the cross sections of the speleothems. With Raman spectroscopy, the following relations of minerals was determined as show in Figure 15. The first observation was that calcite and our opal 1 standard appear to be most present in the part of the speleothem that has grown out past the basalt boundary, with opal 1 being the dominant mineral detected, and calcite occurring less frequently. The chalcedony and the opal 2 standard appear to correlate as well, located predominantly near the basalt-speleothem boundary. The calcite, chalcedony and opal 2 also appear to be more abundant within the basalt boundary where opal 1 is lacking. Assuming that the speleothems grew from within the basalt boundary outwards, it appears that the chalcedony and opal 2 were the silica species that dominated the first part of the speleothem growth along with calcite. Further work will be done to determine what opal 1 and 2 are, however knowing

that the chalcedony was more present in the earlier deposits indicates a more ordered silica species being that amorphous opal is less ordered than chalcedony which is cryptocrystalline (from XRD as well as optical determination). This also might indicate that chalcedony grew at a slightly higher growth rate in comparison to the more amorphous silica and/or in a more acidic environment (Sunagawa, 2005; Gaillou et al., 2008; Kamashev, 2012). By the time that speleothem growth was dominated by opal 1, there might have been a higher concentration of dissolved silica in the water, possibly associated with quicker deposition, lower growth rate, or a more basic environment (Sunagawa, 2005; Gaillou et al., 2008; Kamashev, 2012). It is seen in the present that day that the pH of the waters is slightly basic, typically with a pH of 8-9. This might indicate a change in the cave waters becoming more basic over time. Calcite is seen both in the basalt boundary deposits as well as the speleothem outside of the basalt boundary, perhaps indicating a separate set of growth conditions independent of the influences that act on the silica formation, although pH, temperature and saturation are conditions that affect both minerals forming in caves (Hill and Forti, 1997).

Chalcedony in speleothems is considered rare because crystallization at earth-surface temperature and pressure conditions would take a tremendous amount of time, and its presence has been reported in few cases (Wray, 1999). In quartz sandstone karst caves near Sydney, Australia, Wray (1999) proposed that there is direct transformation of amorphous opal-A to cryptocrystalline chalcedony through the Ostwald paragenetic processes through the dissolution-reprecipitation pathway.

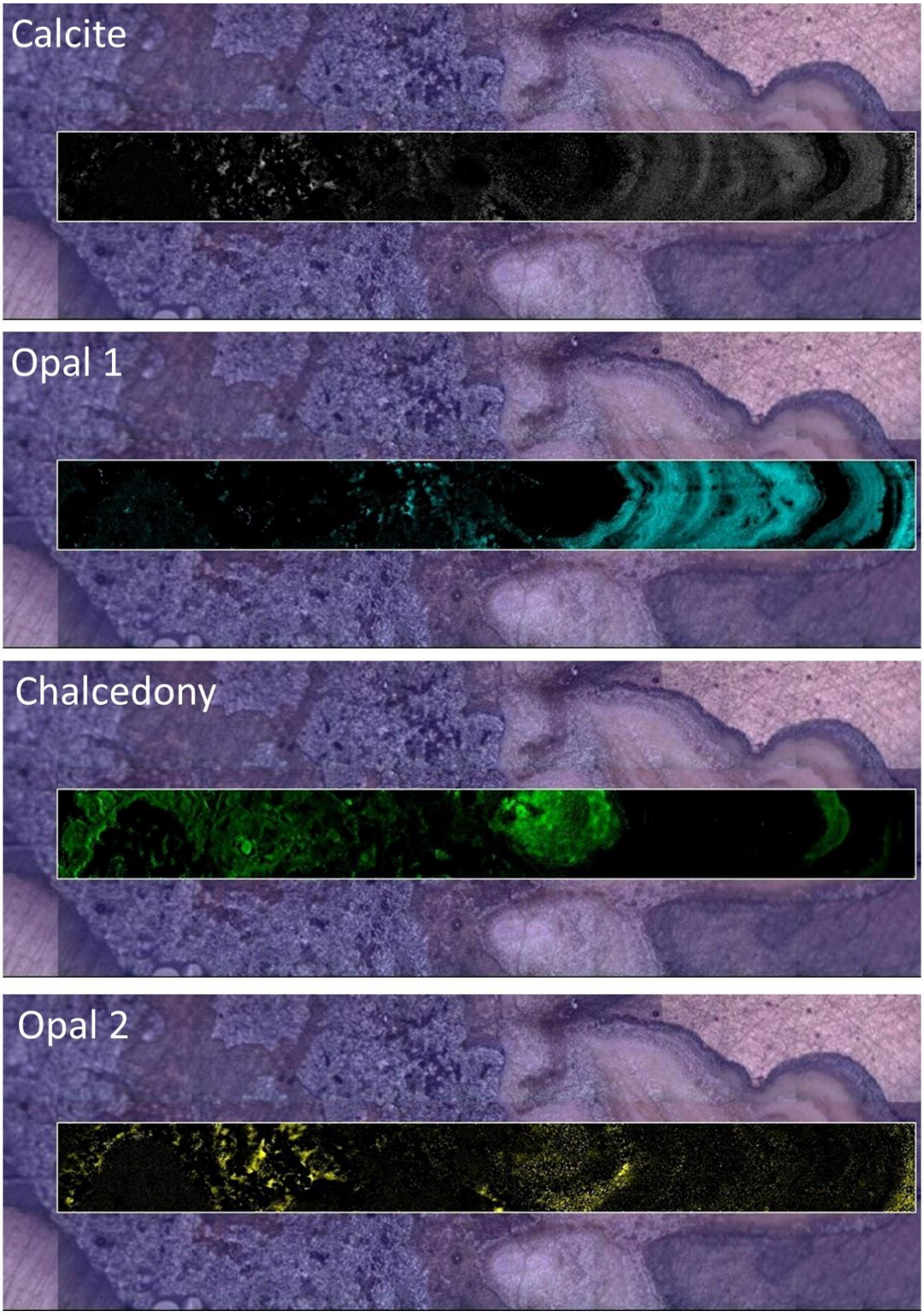

Figure 15 Raman spectra obtained of the speleothem mapped out based on known mineral standards

3.4.2 Organics Mapping

Organics mapping was done through laser-induced fluorescence (LIF). Samples were examined through a line scan across a profile as indicated in Figure 16. Each point in the line scan corresponds to a point spectrum as displayed in Figure 17. Two unique signatures are seen consistently throughout the sample, with peak wavelengths centered at 430 and 310 nm.

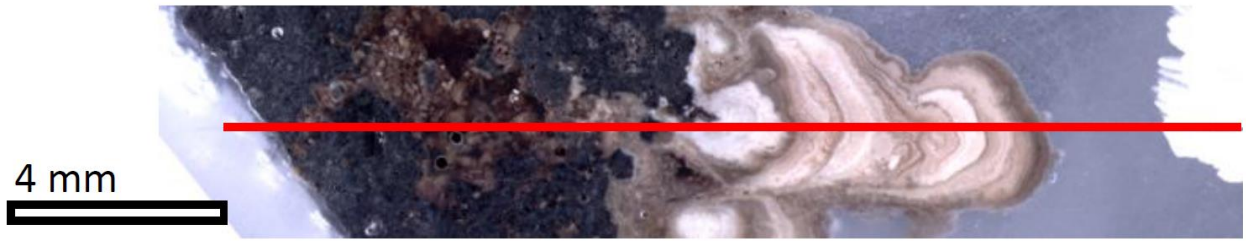

Figure 16 Line scan location in red on speleothem where LIF analysis was conducted

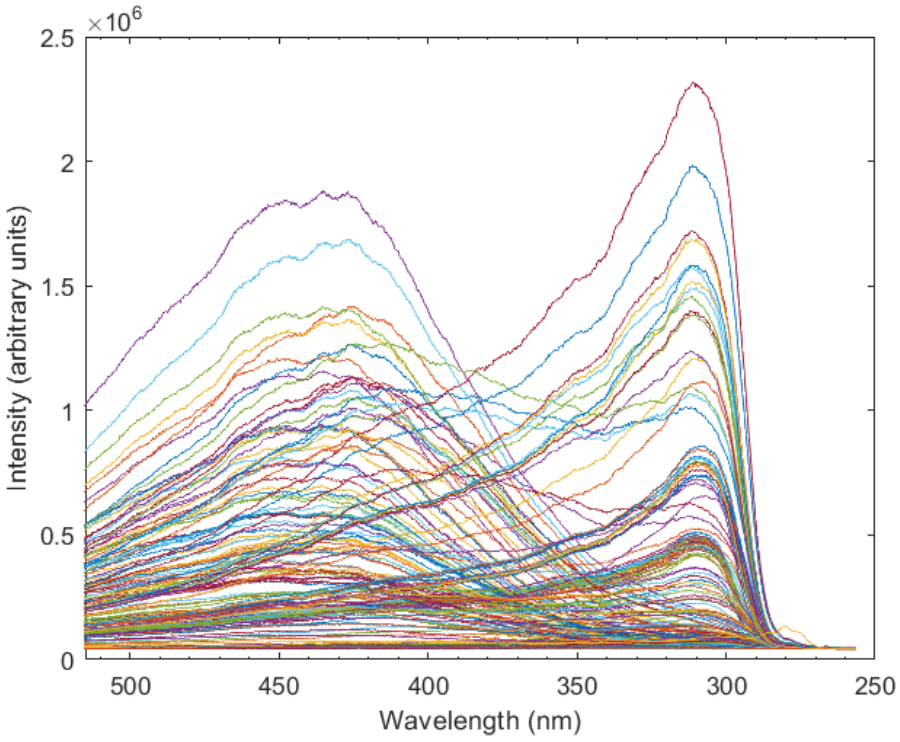

Figure 17 LIF spectra of all points in line scan for fluorescence signature

It has been determined that short-lived (less than 10 ns) fluorescence can be used to differentiate organic fluorescence from mineral fluorescence and could be used as a biosignature (Eshelman et al., 2015). The detection of fluorescence emission in detecting biosignatures and differentiating between organics and minerals is significant compared to current instrumentation in Raman because fluorescence emission occurs on the nanosecond timescale whereas Raman scattering occurs on the femtosecond timescale. Faster fluorescence (less than 10 ns) is likely organic in origin whereas mineral fluorescence usually exhibits longer lived fluorescence due to transition metals or rare earth impurities in minerals (Blacksberg et al., 2010; Gaft and Panczer, 2013; Eshelman, 2016). It is seen in our time-resolved measurements in Figure 18a,b, that we are detecting organic fluorescence. There is also some mineral fluorescence detected in Figure 18a, as shown by the signal that trails on past 10 ns; however, the intensity of the mineral fluorescence is lower compared to the organic fluorescence (the higher peak that decays within 10 ns) where it appears. The majority of the fluorescence signature that is detected in our samples decays well within 10 ns (Figure 18b) and is likely organic in origin.

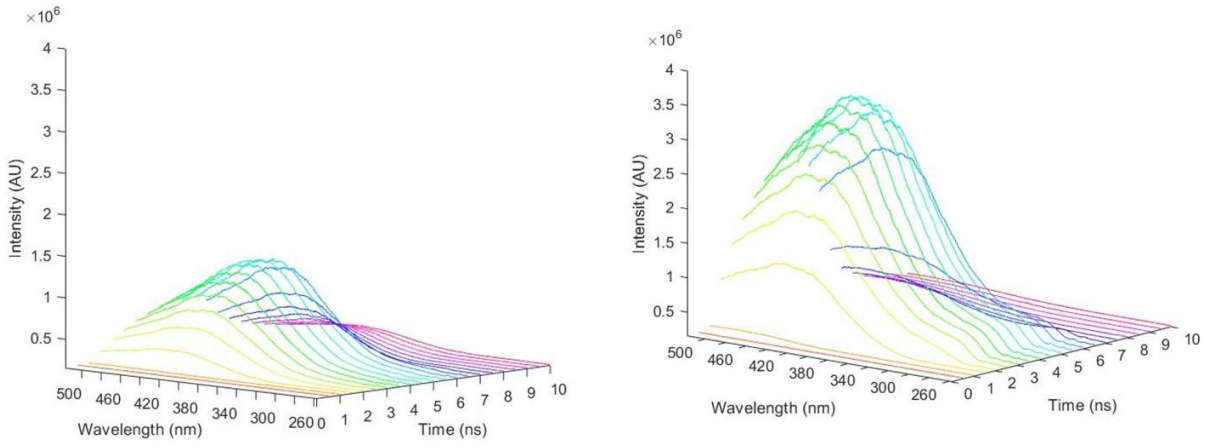

Figure 18 Time resolved measurements taken of points along profile of speleothem. Figure 18a shows both organic fluorescence (peak that decays within the 10 ns) as well as a mineral fluorescence signature that continues past 10 ns. Figure 18b shows fluorescence signature of organic compound that peaks and decays within 10 ns.

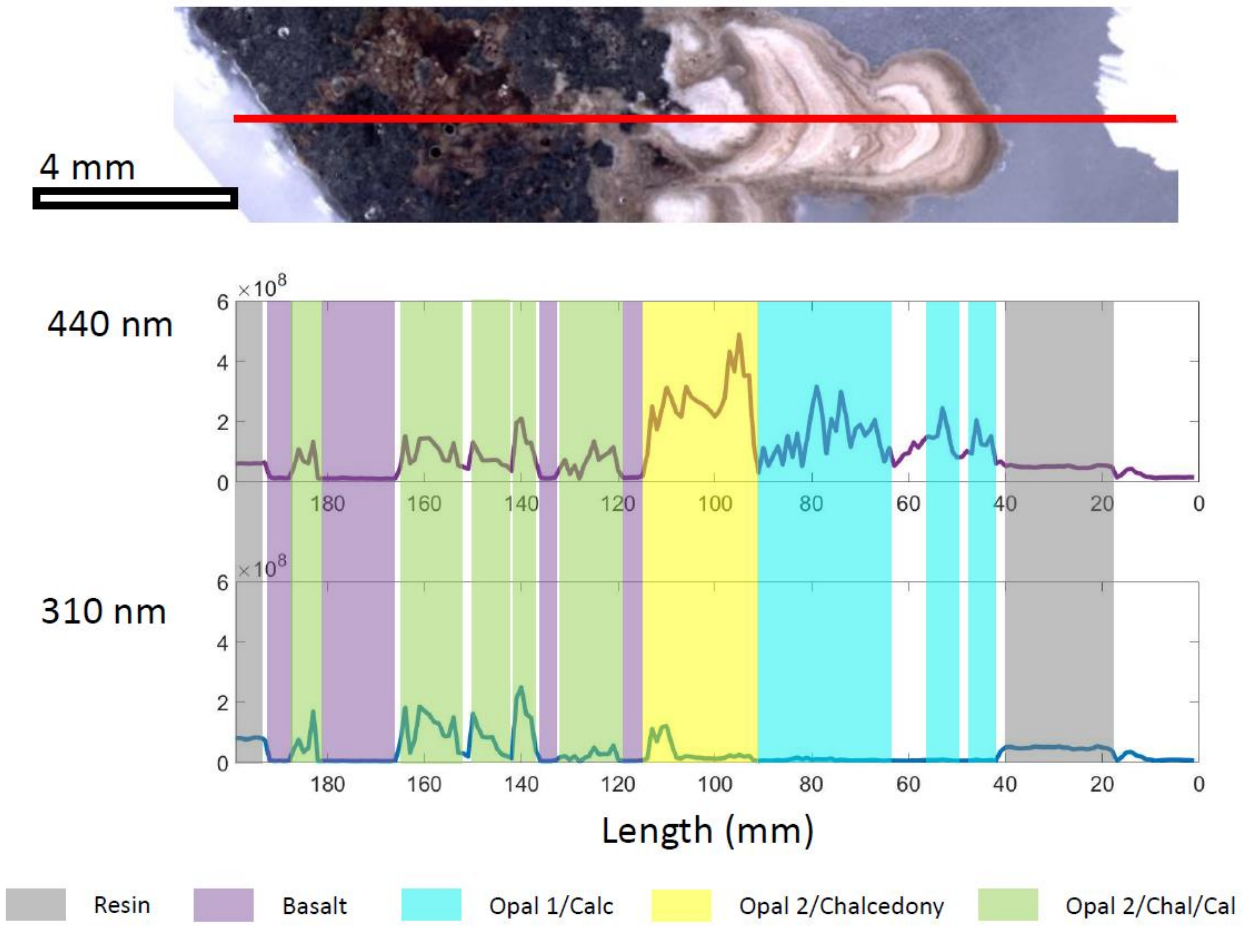

Figure 19 Spatial distribution of fluorescence intensity along the speleothem cross section. Y-axis shows intensity in arbitrary unit from the instrument.

The two unique fluorescence signatures identified in Figure 17 were then examined to see their variation in intensity along the profile. It is seen that basalt shows no fluorescence signature, and that the fluorescence that is detected only correlates to areas where the secondary mineral deposits are (Figure 19). The fluorescence peak at 440 nm is also seen throughout the speleothem sample, with high intensities past the basalt-speleothem boundary. The 310 nm signature is not as prominent past the basalt boundary, with only a minor peak in the area where opal 2 and chalcedony are located. The areas within the basalt boundary where opal 2, chalcedony and calcite are located also seem to contain both fluorescence signatures with near

equal intensities. Comparison of these mineral to organic fluorescence trends suggests that there are two unique signatures that vary spatially along the profile of the speleothem and might be related to the minerals that are there. The occurrence of opal 1 and calcite correlates with the 440 nm fluorescence alone, while opal 2 and chalcedony co-occurs with both fluorescence wavelengths, although 440 nm still dominates. Lastly where opal 2, chalcedony and calcite occur, both fluorescence signatures appear to have similar intensities of fluorescence. Although this suggests some association between the mineral and organics within the speleothem, it is not clear if the two distinct organic signatures are from separate biotic sources, or same source leaving behind different signatures. Further work with GC-MS would help in the understanding of what is actually present, but LIF is an important initial tool that quickly identifies where organic signatures are.

3.5 Conclusion

There is benefit to understanding the relation of minerals to organics where there is direct spatial relation of the two components in the system. Getting a record of the formation history as well as what it records of its environment is useful knowledge even for Earth applications. LIF and Raman are methods which require little sample preparation which can yield a lot of results. Used together, they can provide a lot of information regarding mineral-organic relations. In this study, the use of the two for spatial mapping of a sample showed promise of organic detection. The region with opal 2/chalcedony/calcite that is within the basalt showed similar fluorescence detection in two unique signatures at 440 nm and 310 nm. Fluorescence at 440 nm also proved useful and showed very high intensity fluorescence in areas of opal2/chalcedony grouping as well as opal 1/calcite grouping which were both beyond the basalt boundary. Future work can be

done on more samples to observe trends with different mineral groupings. As well, future work in identifying what the organic compounds are would prove useful in understanding what is being detected.

Summary

With the discovery of lava tubes and hydrologic processes on Mars, it is our hope that there are similar processes of mineral deposits forming in the subsurface on Mars. Studying the mineralogy and geochemistry of these mineral deposits on Earth will hopefully arm us with the best tools to understand and look for biosignatures on Mars. Indications of past life can be very hard to detect and verify but having many different types of analyses detecting different aspects of life (their influence on their environment and chemistry, remnants of their structures, evidence of organic compounds) is an important way to be sure of life detection.

Testing biosignature suites in the preservation of life on Earth will lead us to more efficient detection of life on Mars through proven methods and instrumentation. Lava tubes provide a stable environment for life to not only survive but adapt and proliferate on Earth. On Mars, they provide protection from the harsh surface conditions and might be a good target for astrobiology. From our study, we see that basaltic lava tubes form speleothems that are silica rich. It is especially rich in amorphous silica which has been preserving the microbial structures of the biofilm that coats the exterior of the speleothem. Isotopes have also been an important proxy in understanding source of materials within the cave. We see that in analysing the inorganic and organic components there is an approximately -27.6‰ difference in the two values in aliquots of the same sample. In further analysis on each component in relation to the system, we believe that the organic component might be derived from overlying soil carbon percolating into the cave. The inorganic component is also enriched compared to equilibrium precipitation values, and might be due to kinetic degassing or influence by microbial communities present.

There also appears to be a spatial relation of minerals and organics within the structures seen in cross section of the samples. This could be due to growth of organics and minerals under same environmental influences, or more closely related mechanisms between the minerals and the biofilm. LIF and Raman are instruments that can produce quick and complementary spatial analysis of these different components. They can run analysis on the same samples which is important for correlation of different components in the speleothem. As well, in these samples in LIF unique fluorescence signatures can be isolated and examined in profile. In this case two unique organic signatures were detected peaking at 310 nm and 440 nm. LIF can also within some certainty provide quick information about if the fluorescence detected is organic in origin (short-lived) or if it is mineral.

We recommend further investigation of speleothems for biosignature preservation. Their growth due to hydrologic processes, their intimate relation to biofilms on Earth and their overall reflectance of their environment are all important aspects for astrobiology. We believe further work into other caves, and more detailed analysis of certain aspects summarized in this thesis is important for the use of lava tubes as a planetary analogue. Precise spatial analysis of organic compounds or isotopes in the cross sections of the speleothems would complement the fluorescence and mineral spatial analysis presented in this thesis.

References List

Abramov O. and Kring D. A. (2005) Impact-induced hydrothermal activity on early Mars. *J. Geophys. Res.* **110**, 1–19.

Abrevaya X. C., Anderson R., Arney G., Atri D., Azu A., Bowman J. S., Brazelton W. J., Brennecka G. A., Carns R., Chopra A., Colangelo-lillis J., Crockett C. J., Demarines J., Frank E. A., Frantz C., Fuente E. De, Galante D., Glass J., Gleeson D., Glein C. R., Goldblatt C., Horak R., Horodyskyj L., Knowles E., Mayeur P., Mcglynn S., Miguel Y., Montgomery M., Neish C., Noack L., Rugheimer S., Stu E. E., Tamez-hidalgo P., Walker S. I. and Wong T. (2016) The Astrobiology Primer v2.0. *Astrobiology* **16**, 561–653.

Anderson C. A. (1941) Volcanoes of the Medicine Lake Highland, California. *Bull. Dep. Geol. Sci.* **25**, 347–422.

Aston S. R. (1983) Natural water and atmopheric chemistry of silicon. *Silicon Geochemistry Biogeochem.*, 77–100.

Bandfield J. L., Hamilton V. E. and Christensen P. R. (2000) A global view of Martian surface compositions from MGS-TES. *Science (80-.).* **287**, 1626–1631.

Banerjee N. R., Furnes H., Muehlenbachs K., Staudigel H. and de Wit M. (2006) Preservation of ~ 3.4 – 3.5 Ga microbial biomarkers in pillow lavas and hyaloclastites from the Barberton Greenstone Belt, South Africa. *Earth Planet. Sci. Lett.* **241**, 707–722.

Blacksberg J., Rossman G. R. and Gleckler A. (2010) Time-resolved Raman spectroscopy for in situ planetary mineralogy. *Appl. Opt.*

Bleacher J. E., Greeley R., Williams D. A., Cave S. R. and Neukum G. (2007) Trends in effusive style at the Tharsis Montes, Mars, and implications for the development of the Tharsis province. *J. Geophys. Res.* **112**, 1–15.

Blyth A. J., Hartland A. and Baker A. (2016) Organic proxies in speleothems – New developments, advantages and limitations. *Quat. Sci. Rev.* **149**, 1–17.

Boston P. J., Spilde M. N., Northup D. E., Melim L. A., Soroka D. S., Kleina L. G., Lavoie K. H., Hose L. D., Mallory L. M., Dahm C. N., Crossey L. J. and Schelble R. T. (2001) Cave Biosignature Suites: Microbes, Minerals, and Mars. *Astrobiology* **1**, 30–35.

Brasier M. D., Green O. R., Lindsay J. F., McLoughlin N., Steele A. and Stoakes C. (2005) Critical testing of Earth's oldest putative fossil assemblage from the ~3.5 Ga Apex chert, Chinaman Creek, Western Australia. *Precambrian Res.*

Buatois L. A., Renaut R. W., Scott J. J. and Bernhart Owen R. (2017) An unusual occurrence of the trace fossil Vagorichnus preserved in hydrothermal silica at Lake Baringo, Kenya Rift Valley: Taphonomic and paleoenvironmental significance. *Palaeogeogr. Palaeoclimatol. Palaeoecol.* **485**, 843–853.

Cabrol N. A., Grin E. A. and Wynne J. J. (2009) Detection of caves and cave-bearing geology on Mars. In *40th Lunar and Planetary Science Conference* p. Abstract No. 1040.

Caddeo G. A., Railsback L. B., Waele J. De and Frau F. (2015) Stable isotope data as constraints on models for the origin of coralloid and massive speleothems: The interplay of substrate, water supply, degassing, and evaporation. *Sediment. Geol.* **318**, 130–141.

Cady S. L., Farmer J. D., Grotzinger J. P., Schopf J. W. and Steele A. (2003) Morphological Biosignatures and the Search for Life on Mars. *Astrobiology* **3**, 351–368.

Calvari S. and Pinkerton H. (1999) Lava tube morphology on Etna and evidence for lava flow emplacement mechanisms. *J. Volcanol. Geotherm. Res.* **90**, 263–280.

Carter J., Loizeau D., Mangold N., Poulet F. and Bibring J.-P. (2015) Widespread surface weathering on early Mars: A case for a warmer and wetter climate. *Icarus* **248**, 373–382.

Cattermole P. (1990) Volcanic Flow Development at Alba Patera, Mars. *Icarus* **83**, 453–493.

Coleman N. M., Dinwiddie C. L. and Casteel K. (2007) High outflow channels on Mars indicate Hesperian recharge at low latitudes and the presence of Canyon Lakes. *Icarus* **189**, 344–361.

Crown D. A. and Ramsey M. S. (2017) Morphologic and thermophysical characteristics of lava flows southwest of Arsia Mons, Mars. *J. Volcanol. Geotherm. Res.* **342**, 13–28. Available at: http://dx.doi.org/10.1016/j.jvolgeores.2016.07.008.

Cushing G. E. (2012) Candidate cave entrances on Mars. *J. Cave Karst Stud.* **74**, 33–47.

DiPaolo D. A., Smith S. B., Odion D. C., Ives J. H. and Sarr D. A. (2015) *Vegetation Classification and Mapping: Lava Beds National Monument*., National Park Service.

Donnelly-Nolan J. D. and Lanphere M. A. (2005) U.S. Geological Survey Open-File Report. In *U.S. Geological Survey Open-File Report*

Donnelly-Nolan J. M. (2010) *Geologic Map of Medicine Lake Volcano, Northern California*., US Geological Survey

Donnelly-Nolan J. M. and Champion D. E. (1987) Geologic map of Lava Beds National Monument, Northern California. US Geological Survey

Donnelly-Nolan J. M., Grove T. L., Lanphere M. A., Champion D. E. and Ramsey D. W. (2008) Eruptive history and tectonic setting of Medicine Lake Volcano, a large rear-arc volcano in the southern Cascades. *J. Volcanol. Geotherm. Res.* **177**, 313–328.

Ehlmann B. L., Mustard J. F., Murchie S. L., Bibring J., Meunier A., Fraeman A. A. and Langevin Y. (2011) Subsurface water and clay mineral formation during the early history of Mars. *Nature* **479**, 53–60.

Eshelman E., Daly M. G., Slater G. and Cloutis E. (2015) Time-resolved detection of aromatic compounds on planetary surfaces by ultraviolet laser induced fluorescence and Raman spectroscopy. *Planet. Space Sci.* **119**, 200–207.

Eshelman E., Daly M. G., Slater G., Dietrich P. and Gravel J. F. (2014) An ultraviolet Raman wavelength for the in-situ analysis of organic compounds relevant to astrobiology. *Planet. Space Sci.* **93**–**94**, 65–70.

Eshelman E. J. (2016) Stand-Off Detection of Organic Compounds on Mars Using Ultraviolet Raman Spectroscopy and Time-Resolved Laser-Induced Fluorescence.

Fliegel D., Kosler J., McLoughlin N., Simonetti A., de Wit M. J., Wirth R. and Furnes H. (2010) In-situ dating of the Earth's oldest trace fossil at 3.34 Ga. *Earth Planet. Sci. Lett.* **299**, 290–298.

De Freitas C. R., Littlejohn R. N., Clarkson T. S. and Kristament I. S. (1982) Cave climate: assessment of airflow and ventilation. *J. Climatol.* **2**, 383–397.

Gaft M. and Panczer G. (2013) Laser-induced time-resolved luminescence spectroscopy of minerals: A powerful tool for studying the nature of emission centres. *Mineral. Petrol.*

Gaillou E., Fritsch E., Aguilar-Reyes B., Rondeau B., Post J., Barreau A. and Ostroumov M. (2008) Common gem opal: An investigation of micro- to nano-structure. *Am. Mineral.* **93**, 1865–1873.

Greenough J. D. and Ya'acoby A. (2013) A comparative geochemical study of Mars and Earth basalt petrogenesis. *Can. J. Earth Sci.* **50**, 78–93.

Grin E. A., Cabrol N. A. and McKay C. P. (1998) Caves in the Martian regolith and their significance for exobiology exploration. In *29th Lunar and Planetary Science Conference* p. Abstract No. 1012.

Hathaway J. J. M., Garcia M. G., Balasch M. M., Spilde M. N., Stone F. D., Dapkevicius M. de L., Amorim I. R., Gabriel R., Borges P. A. V and Northup D. E. (2014) Comparison of bacterial diversity in Azorean and Hawai'ian lava cave microbial mats. *Geomicrobiol. J.* **31**, 205–220.

Herdianita N. R., Browne P. R. L., Rodgers K. A. and Campbell K. A. (2000) Mineralogical and textural changes accompanying ageing of silica sinter. *Miner. Depos.* **35**, 48–62.

Hill C. A. and Forti P. (1997) *Cave Minerals of the World*. 2nd ed., National Speleological Society, Huntsville, AL.

Ingraham N. L. and Taylor B. E. (1991) Light stable isotope systematics of large-scale hydrologic regimes in California and Nevada. *Water Resour. Res.* **27**, 77–90.

Jones B. (2001) Microbial activity in caves - A geological perspective. *Geomicrobiol. J.* **18**, 345–357.

Jones B. and Motyka A. (1987) Biogenic structures and micrite in stalactites from Grand Cayman Island, British West Indies. *Can. J. Earth Sci.* **24**, 1402–1411.

Jones J. B., Sanders J. V. and Segnit E. R. (1964) Structure of Opal. *Nature* **204**, 990–991.

Jung J., Hong I. S., Cho E. and Yi Y. (2016) Method for identifying lava tubes among pit craters using brightness profile across pits on the moon or mars. *J. Astron. Sp. Sci.* **33**, 21–28.

Kamashev D. V. (2012) Synthesis, properties, and model of the formation of silica supramolecular structures. *Glas. Phys. Chem.* **38**, 307–314.

Keszthelyi L. (1995) A preliminary thermal budget for lava tubes on the Earth and planets. *J. Geophys. Res.* **100**, 411–420.

Keszthelyi L., Self S. and Thordarson T. (2006) Flood lavas on Earth, Io and Mars. *J. Geol. Soc. London* **163**, 253–264.

Kidder D. L. and Erwin D. H. (2001) Secular distribution of biogenic silica through the Phanerozoic: Comparison of silica-replaced fossils and bedded cherts at the series level. *J. Geol.* **109**, 509–522.

Kim S.-T. and O'Neil J. R. (1997) Equilibrium and nonequilibrium oxygen isotope effects in synthetic carbonates. *Geochim. Cosmochim. Acta* **61**, 3461–3475.

Knoll A. H., Bergmann K. D. and Strauss J. V. (2016) Life: The first two billion years. *Philos. Trans. R. Soc. B Biol. Sci.* **371**.

Lachniet M. S. (2009) Climatic and environmental controls on speleothem oxygen-isotope values. *Quat. Sci. Rev.* **28**, 412–432.

Lavoie K. H., Winter A. S., Read K. J. H., Hughes E. M., Spilde M. N. and Northup D. E. (2017) Comparison of bacterial communities from lava cave microbial mats to overlying surface soils from Lava Beds National Monument, USA. *PLoS One* **12**, 1–27.

Lennon J. T., Nguyễn-Thùy D., Phạm T. M., Drobniak A., Tạ P. H., Phạm N., Streil T., Webster K. D. and Schimmelmann A. (2017) Microbial contributions to subterranean methane sinks. *Geobiology* **15**, 254–258.

Leone G. (2014) A network of lava tubes as the origin of Labyrinthus Noctis and Valles Marineris on Mars. *J. Volcanol. Geotherm. Res.* **277**, 1–8.

Léveillé R. (2010) A half-century of terrestrial analog studies: From craters on the Moon to searching for life on Mars. *Planet. Space Sci.* **58**, 631–638.

Léveillé R. J. and Datta S. (2010) Lava tubes and basaltic caves as astrobiological targets on Earth and Mars: A review. *Planet. Space Sci.* **58**, 592–598.

Léveillé R. J., Longstaffe F. J. and Fyfe W. S. (2007) An isotopic and geochemical study of carbonate-clay mineralization in basaltic caves: abiotic versus microbial processes. *Geobiology* **5**, 235–249.

Léveillé R. J., Longstaffe F. J. and Fyfe W. S. (2002) Kerolite in carbonate-rich speleothems and microbial deposits from basaltic caves, Kauai, Hawaii. *Clays Clay Miner.* **50**, 514–524.

Liesegang M., Milke R. and Berthold C. (2018) Amorphous silica maturation in chemically weathered clastic sediments. *Sediment. Geol.* **365**, 54–61.

Miller A. Z., De la Rosa J. M., Jiménez-Morillo N. T., Pereira M. F. C., González-Pérez J. A., Calaforra J. M. and Saiz-Jimenez C. (2016) Analytical pyrolysis and stable isotope analyses

reveal past environmental changes in coralloid speleothems from Easter Island (Chile). *J. Chromatogr. A* **1461**, 144–152.

Miller A. Z., Pereira M. F. C., Calaforra J. M., Forti P., Amélia D. and Saiz-Jimenez C. (2014) Siliceous speleothems and associated microbe-mineral interactions from Ana Heva lava tube in Easter Island (Chile). *Geomicrobiol. J.* **31**, 236–245.

Mulugeta L., Battler M. M., Kobrick R. L., Thaler J., Shelaga R. and Persaud R. (2011) Expedition Mars: A Mars analogue program dedicated to advancing competency in human planetary surface exploration. In *International Conference on Environmental Systems*

Natelhoffer K. J. and Fry B. (1988) Controls on natural nitrogen-15 and carbon-13 abundances in forest soil organic matter. *Soil Sci. Soc. Am. J.* **52**, 1633–1640.

Nathenson M., Donnelly-Nolan J. M., Champion D. E. and Lowenstern J. B. (2007) *Chronology of Postglacial Eruptive Activity and Calculation of Eruption Probabilities for Medicine Lake Volcano, Northern California*., US Geological Survey.

Niles P. B., Catling D. C., Berger G., Chassefière E., Ehlmann B. L., Michalski J. R., Morris R., Ruff S. W. and Sutter B. (2013) Geochemistry of carbonates on Mars: Implications for climate history and nature of aqueous environments. *Space Sci. Rev.* **174**, 301–328.

Northup D. E. and Lavoie K. H. (2001) Geomicrobiology of caves: A review. *Geomicrobiol. J.* **18**, 199–222.

Northup D. E., Melim L. A., Spilde M. N., Hathaway J. J. M., Garcia M. G., Moya M., Stone F. D., Boston P. J., Dapkevicius M. L. N. E. and Riquelme C. (2011) Lava cave microbial communities within mats and secondary mineral deposits: implications for life detection on other planets. *Astrobiology* **11**, 601–618.

Parmentier E. M. and Zuber M. T. (2007) Early evolution of Mars with mantle compositional stratification or hydrothermal crustal cooling. *J. Geophys. Res.* **112**, 1–11.

Perry R. W. (2013) A review of factors affecting cave climates for hibernating bats in temperate North America. *Environ. Rev.* **21**, 28–39.

Perşoiu A. and Pazdur A. (2011) Ice genesis and its long-term mass balance and dynamics in Scărişoara Ice Cave, Romania. *Cryosph.* **5**, 45–53.

Peterson D. W., Holcomb R. T., Tilling R. I. and Christiansen R. L. (1994) Development of lava tubes in the light of observations at Mauna Ulu, Kilauea Volcano, Hawaii. *Bull. Volcanol.* **56**, 343–360.

Piret F. and Su B. L. (2008) Effects of pH and ionic strength on the self-assembly of silica colloids to opaline photonic structures. *Chem. Phys. Lett.* **457**, 376–380.

Preston L. J., Benedix G. K., Genge M. J. and Sephton M. A. (2008) A multidisciplinary study of silica sinter deposits with applications to silica identification and detection of fossil life on Mars. *Icarus* **198**, 331–350.

Racovita G. and Onac B. P. (2000) *Scarisoara Glacier Cave Monographic study*., Editura Carpatica.

Raes J. (2010) Crowdsourcing Earth's microbes. *Nature* **551**, 446–447.

Reid R. P., Visscher P. T., Decho A. W., Stolz J. F., Bebout B. M., Dupraz C., Macintyre I. G., Paerl H. W., Pinckney J. L., Prufert-Bebout L., Steppe T. F. and DesMarais D. J. (2000) The role of microbes in accretion, lamination and early lithifacation of modern stromatolites. , 989–992.

Riquelme C., Rigal F., Hathaway J. J. M., Northup D. E., Spilde M. N., Borges P. A. V., Gabriel R., Amorim I. R. and Dapkevicius M. D. L. N. E. (2015) Cave microbial community composition in oceanic islands: disentangling the effect of different colored mats in diversity patterns of Azorean lava caves. *FEMS Microbiol. Ecol.* **91**, 1–12.

Rowland S. K., Harris A. J. L. and Garbeil H. (2004) Effects of Martian conditions on numerically modeled, cooling-limited, channelized lava flows. *J. Geophys. Res.* **109**, E10010 1-16.

Rummel J. D. (2005) Planetary protection and human Mars exploration: Precursor and analogue studies. In *International Astronautical Congress*

Schopf J. W. (1993) Microfossils of the early Archean apex chert: New evidence of the antiquity of life. *Science (80-.).* **260**, 640–646.

Schubert J. K., Kidder D. L. and Erwin D. H. (1997) Silica-replaced fossils through the Phanerozoic. *Geology* **25**, 1031–1034.

Schwenzer S. P., Abramov O., Allen C. C., Bridges J. C., Clifford S. M., Filiberto J., Kring D. A., Lasue J., Mcgovern P. J., Newsom H. E., Treiman A. H., Vaniman D. T., Wiens R. C. and Wittmann A. (2012) Gale Crater: Formation and post-impact hydrous environments. *Planet. Space Sci.* **70**, 84–95.

Senkayi A. L., Dixon J. B., Hossner L. R., Yerima B. P. K. and Wilding L. P. (1985) Replacement of quartz by opaline silica during weathering of petrified wood. *Clays Clay Miner.* **33**, 525–531.

Sumner D. Y. (2001) Microbial influences on local carbon isotopic ratios and their preservation in carbonate. *Astrobiology* **1**, 57–70.

Sunagawa I. (2005) *Crystals: Growth, morphology, and perfection*., Cambridge University Press.

Thompson L. R., Sanders J. G., McDonald D., Amir A., Ladau J., Locey K. J., Prill R. J., Tripathi A., Gibbons S. M., Ackermann G., Navas-Molina J. A., Janssen S., Kopylova E., Vázquez-Baeza Y., González A., Morton J. T., Mirarab S., Zech Xu Z., Jiang L., Haroon M. F., Kanbar J., Zhu Q., Jin Song S., Kosciolek T., Bokulich N. A., Lefler J., Brislawn C. J., Humphrey G., Owens S. M., Hampton-Marcell J., Berg-Lyons D., McKenzie V., Fierer N., Fuhrman J. A., Clauset A., Stevens R. L., Shade A., Pollard K. S., Goodwin K. D., Jansson J. K., Gilbert J. A., Knight R., Consortium T. E. M. P., Rivera J. L. A., Al-Moosawi L., Alverdy J., Amato K. R., Andras J., Angenent L. T., Antonopoulos D. A., Apprill A., Armitage D., Ballantine K., Bárta J., Baum J.

K., Berry A., Bhatnagar A., Bhatnagar M., Biddle J. F., Bittner L., Boldgiv B., Bottos E., Boyer D. M., Braun J., Brazelton W., Brearley F. Q., Campbell A. H., Caporaso J. G., Cardona C., Carroll J., Cary S. C., Casper B. B., Charles T. C., Chu H., Claar D. C., Clark R. G., Clayton J. B., Clemente J. C., Cochran A., Coleman M. L., Collins G., Colwell R. R., Contreras M., Crary B. B., Creer S., Cristol D. A., Crump B. C., Cui D., Daly S. E., Davalos L., Dawson R. D., Defazio J., Delsuc F., Dionisi H. M., Dominguez-Bello M. G., Dowell R., Dubinsky E. A., Dunn P. O., Ercolini D., Espinoza R. E., Ezenwa V., Fenner N., Findlay H. S., Fleming I. D., Fogliano V., Forsman A., Freeman C., Friedman E. S., Galindo G., Garcia L., Garcia-Amado M. A., Garshelis D., Gasser R. B., Gerdts G., Gibson M. K., Gifford I., Gill R. T., Giray T., Gittel A., Golyshin P., Gong D., Grossart H.-P., Guyton K., Haig S.-J., Hale V., Hall R. S., Hallam S. J., Handley K. M., Hasan N. A., Haydon S. R., Hickman J. E., Hidalgo G., Hofmockel K. S., Hooker J., Hulth S., Hultman J., Hyde E., Ibáñez-Álamo J. D., Jastrow J. D., Jex A. R., Johnson L. S., Johnston E. R., Joseph S., Jurburg S. D., Jurelevicius D., Karlsson A., Karlsson R., Kauppinen S., Kellogg C. T. E., Kennedy S. J., Kerkhof L. J., King G. M., Kling G. W., Koehler A. V, Krezalek M., Kueneman J., Lamendella R., Landon E. M., Lane-deGraaf K., LaRoche J., Larsen P., Laverock B., Lax S., Lentino M., Levin I. I., Liancourt P., Liang W., Linz A. M., Lipson D. A., Liu Y., Lladser M. E., Lozada M., Spirito C. M., MacCormack W. P., MacRae-Crerar A., Magris M., Martín-Platero A. M., Martín-Vivaldi M., Martínez L. M., Martínez-Bueno M., Marzinelli E. M., Mason O. U., Mayer G. D., McDevitt-Irwin J. M., McDonald J. E., McGuire K. L., McMahon K. D., McMinds R., Medina M., Mendelson J. R., Metcalf J. L., Meyer F., Michelangeli F., Miller K., Mills D. A., Minich J., Mocali S., Moitinho-Silva L., Moore A., Morgan-Kiss R. M., Munroe P., Myrold D., Neufeld J. D., Ni Y., Nicol G. W., Nielsen S., Nissimov J. I., Niu K., Nolan M. J., Noyce K., O'Brien S. L., Okamoto N., Orlando L., Castellano Y. O., Osuolale O., Oswald W., Parnell J., Peralta-Sánchez J. M., Petraitis P., Pfister C., Pilon-Smits E., Piombino P., Pointing S. B., Pollock F. J., Potter C., Prithiviraj B., Quince C., Rani A., Ranjan R., Rao S., Rees A. P., Richardson M., Riebesell U., Robinson C., Rockne K. J., Rodriguezl S. M., Rohwer F., Roundstone W., Safran R. J., Sangwan N., Sanz V., Schrenk M., Schrenzel M. D., Scott N. M., Seger R. L., Seguin-Orlando A., Seldin L., Seyler L. M., Shakhsheer B., Sheets G. M., Shen C., Shi Y., Shin H., Shogan B. D., Shutler D., Siegel J., Simmons S., Sjöling S., Smith D. P., Soler J. J., Sperling M., Steinberg P. D., Stephens B., Stevens M. A., Taghavi S., Tai V., Tait K., Tan C. L., Tas¸ N., Taylor D. L., Thomas T., Timling I., Turner B. L., Urich T., Ursell L. K., van der Lelie D., Van Treuren W., van Zwieten L., Vargas-Robles D., Thurber R. V., Vitaglione P., Walker D. A., Walters W. A., Wang S., Wang T., Weaver T., Webster N. S., Wehrle B., Weisenhorn P., Weiss S., Werner J. J., West K., Whitehead A., Whitehead S. R., Whittingham L. A., Willerslev E., Williams A. E., Wood S. A., Woodhams D. C., Yang Y., Zaneveld J., Zarraonaindia I., Zhang Q. and Zhao H. (2017) A communal catalogue reveals Earth's multiscale microbial diversity. *Nature* **551**, 457.

Tomczyk-Żak K. and Zielenkiewicz U. (2016) Microbial Diversity in Caves. *Geomicrobiol. J.* **33**, 20–38.

Toporski J. K. W., Steele A., Westall F., Thomas-Keprta K. L. and Mckay D. S. (2002) The simulated silicification of bacteria — New clues to the modes and timing of bacterial preservation and implications for the search for extraterrestrial microfossils. *Astrobiology* **2**, 1–26.

Torres M., Niell F. X. and Algarra P. (1991) Photosynthesis of Gelidium sesquipedale: effects of temperature and light on pigment concentration, C/N ratio and cell-wall polysaccharides. *Hydrobiologia* **221**, 77–82.

Urey H. C. (1952) *The Planets. Their Origin and Development.,* Yale University Press.

Vanghi V., Frisia S. and Borsato A. (2017) Genesis and microstratigraphy of calcite coralloids analysed by high resolution imaging and petrography. *Sediment. Geol.* **359**, 16–28.

Waters A. C., Donnelly-Nolan J. M. and Rogers B. W. (1990) *Selected caves and lava-tube systems in and near Lava Beds National Monument, California*.

Webster K. D., Mirza A., Deli J. M., Sauer P. E. and Schimmelmann A. (2016) Consumption of atmospheric methane in a limestone cave in Indiana, USA. *Chem. Geol.* **443**, 1–9.

Williams K. E., Mckay C. P., Toon O. B. and Head J. W. (2010) Do ice caves exist on Mars? *Icarus* **209**, 358–368.

Woo K. S. (2005) *Caves: A Wonderful Underground*., Hollym International Corporation.

Woo K. S., Choi D. W. and Lee K. C. (2008) Silicification of cave corals from some lava tube caves in the Jeju Island, Korea: Implications for speleogenesis and a proxy for paleoenvironmental change during the Late Quaternary. *Quat. Int.* **176**–**177**, 82–95.

Wray R. A. L. (1999) Opal and chalcedony speleothems on quartz sandstones in the Sydney region, southeastern Australia. *Aust. J. Earth Sci.* **46**, 623–632.

Wu X., Zhu X., Pan M. and Zhang M. (2015) Dissolved inorganic carbon isotope compositions of drip water in Panlong cave, southwest China. *Environ. Earth Sci.* **74**, 1029–1037.

Wyrick D., Ferrill D. A. and Morris A. P. (2004) Distribution, morphology, and origins of Martian pit crater chains. *J. Geophys. Res.* **109**, 20.

Yonge C. J. and MacDonald W. D. (1999) The potential of perennial cave ice in isotope palaeoclimatology. *Boreas* **28**, 357–362.